Charmless charged two-body B decays at LHCb

Public Note

Issue:	1
Revision:	0
Reference:	CERN-LHCb-2007-059
Created:	February 13, 2007
Last modified:	September 8, 2007

Prepared by: A. Carbone[1], J. Nardulli[2], S. Pennazzi[3], A. Sarti[4], V. Vagnoni[1]

[1]*INFN, Sezione di Bologna, Italy*
[2]*NIKHEF, Amsterdam, The Netherlands*
[3]*INFN, Sezione di Firenze, Italy*
[4]*INFN, Laboratori Nazionali di Frascati, Italy*

Abstract

In this note we summarize the status of the studies on charmless charged two-body B-meson decays at LHCb. LHCb has a great potential for triggering, reconstructing and selecting a huge number of such decays, increasing the available statistics from the B-factories and the Tevatron by more than one order of magnitude. First we will describe the selection algorithm and its performance, then we will show how it is possible to get relevant information on the γ angle of the Unitarity Triangle and on the breaking of the U-spin symmetry using these decays.

Document Status Sheet

1. Document Title: Charmless charged two-body B decays at LHCb			
2. Document Reference Number: CERN-LHCb-2007-059			
3. Issue	4. Revision	5. Date	6. Reason for change
Draft	1	February, 2007	First version.

Contents

List of Figures

List of Tables

1 Introduction

The charmless decays of B-mesons to two-body modes have been extensively studied and are still a matter of great interest at the B-factories and the Tevatron. Even if the current knowledge in the B_d/B_u sectors starts to be quite constrained, the B_s sector still remains a field where a rich programme of physics can be pursued.

At present, by using a displaced vertex trigger, CDF has already collected important samples of $B \to h^+h'^-$ decays (1), providing the first observations of the two-body modes $B_s \to K^+K^-$ and $B_s \to \pi^+K^-$. Very soon CDF will obtain the first time dependent CP-violation measurements with these channels. This fact has interesting consequences for LHCb, since it clearly demonstrates that it is possible, although more difficult with respect to the clean environment of the B-factories, to make precision physics measurements in the B-meson sector at hadronic machines. The objectives at the

Charmless charged two-body B decays at LHCb   **Ref:** *CERN-LHCb-2007-059*
Public Note   **Issue:** *1*
2   Reconstruction and selection of $B \to h^+ h'^-$ decays   **Date:** *September 8, 2007*

Tevatron are in fact to obtain, for many channels, sensitivities similar to the B-factory ones at the end of the data taking, i.e. with an integrated luminosity of 6-8 fb^{-1} per experiment, to be compared to 1 ab^{-1} expected at each of the two B-factories running at the $\Upsilon(4S)$ (most probably a bit less for BaBar).

LHCb, thanks to the large beauty production cross section at the LHC, expected to be around $500~\mu b$, and to its excellent vertexing (2) and triggering (3) capabilities, will be able to collect huge samples of $B \to h^+ h'^-$ decays, of the order of about 200k per 2 fb^{-1} of integrated luminosity, roughly corresponding to 1 year of data taking. Furthermore, its particle identification system, notably including two RICH detectors, will allow it to disentangle the various $B \to h^+ h'^-$ modes with a purity exceeding 90%, as well as high efficiency.

In the following sections we will give a description of the event selection procedure. We will also show some studies on the systematic effects due to the variation of the momentum resolution and on the particle ID calibration. Then we will report the results of a sensitivity study on time-dependent CP violation measurements, and finally we will briefly describe how to get from these decays interesting insights into CKM physics as well as hadron dynamics.

2   Reconstruction and selection of $B \to h^+ h'^-$ decays

2.1   Monte Carlo samples

In order to define the selection criteria, different Monte Carlo samples produced with the so-called *DC04* LHCb mass production (4) have been analyzed. They are summarized in Tab. 1. In the same table we also report the branching ratios assumed for each decay mode. The values of the probabilities that b-quarks hadronize to the B-hadrons of interest are shown in Tab. 2.

The Monte Carlo events were generated by the PYTHIA event generator (5), and then processed by means of GEANT4 (6) in order to simulate the detector response. These two steps were performed by the LHCb simulation program Gauss (7), version v15r13 for the $b\bar{b}$-inclusive sample and v15r19 for the signal decay samples. The digitization of the GEANT4 output was then realized by the LHCb digitization program Boole (8), version v5r9 for the $b\bar{b}$-inclusive sample and v6r5 for the signal decay samples. The simulation and digitization included realistic material description, pile-up and spill-over effects, detection efficiencies and resolutions from beam tests of prototypes, electronic noise and cross-talk. The reconstruction was performed by the LHCb reconstruction program Brunel (9), version v23r7 for the $b\bar{b}$-inclusive sample and v24r5 for the signal decay samples, using realistic pattern recognition algorithms. The trigger response was also simulated. Finally, the analysis of reconstructed events was performed by means of the LHCb analysis program DaVinci (10), version v12r14. Monte Carlo truth information was not used in any step of the generation-digitization-trigger-reconstruction-analysis chain.

In order to save computing time, Monte Carlo events have been generated with an acceptance cut at the generator level. For signal events, the cut consists in requiring that the B-hadron of interest decays in the forward direction[1], inside a cone having an opening angle of 400 mrad. This discards B-hadrons flying largely outside the LHCb acceptance as in this case it would be kinematically impossible that all the decay products of an exclusive decay mode could go into the detector acceptance. For $b\bar{b}$-inclusive events, the generator cut is slightly different, since it consists in requiring that *at least* one of the two B-hadrons in the event lies inside the acceptance cone of 400 mrad. The efficiencies due to these generator level cuts need to be accounted for when calculating event yields and background-to-signal ratios. They are reported in Tab. 3.

---

[1]According to the full forward-backward symmetry of the problem, in the case that the interesting B-hadron is generated flying to the backward direction, the whole event is spatially reflected to save computing time.

Charmless charged two-body B decays at LHCb
Public Note
2   Reconstruction and selection of $B \to h^+h'^-$ **decays**

Ref: *CERN-LHCb-2007-059*
Issue: *1*
Date: *September 8, 2007*

Channel	Monte Carlo Analyzed events	Branching ratio $\times 10^6$
$B_d \to \pi^+\pi^-$	41500	4.8
$B_d \to K^+\pi^-$	160000	18.5
$B_s \to \pi^+ K^-$	10500	4.8
$B_s \to K^+ K^-$	40000	18.5
$\Lambda_b \to p\pi^-$	10500	4.8
$\Lambda_b \to pK^-$	40000	18.5
bb-inclusive	27288409	−

Table 1 Number of Monte Carlo events analyzed to optimize the event selection and to evaluate the yields and background-to-signal ratios of the $B \to h^+h'^-$ and $\Lambda_b \to ph^-$ decays reconstructed at LHCb. The last column contains the assumed branching fractions, corresponding to the knowledge at the time of these studies, i.e. not including the most recent measurements from the B-factories and the Tevatron.

B hadron	Hadronization factor (HFAG)	Fraction produced in the Monte Carlo events
B_d, $B^\pm$	$(39.9 \pm 1.0)\%$	40.5%
B_s	$(10.2 \pm 1.4)\%$	9.9%
b baryon	$(10.0 \pm 1.7)\%$	9.1%

Table 2 Hadronization probabilities for the b-quarks to form the B-hadrons of interest: HFAG averages (11) and values used in the simulation.

Particle	Efficiency of 400 *mrad* cut
B_d	$(35.5 \pm 0.4)\%$
$\overline{B}_d$	$(34.2 \pm 0.4)\%$
B_s	$(34.3 \pm 0.4)\%$
$\overline{B}_s$	$(35.3 \pm 0.4)\%$
B^+	$(34.7 \pm 0.4)\%$
B^-	$(35.1 \pm 0.4)\%$
Λ_b	$(34.7 \pm 0.4)\%$
$\overline{\Lambda}_b$	$(34.6 \pm 0.4)\%$
bb-inclusive	$(43.4 \pm 0.3)\%$

Table 3 Generation efficiencies, taking into account the 400 mrad forward cut on the value of the production polar angle of the *b*-hadron coming from the primary collision.

Charmless charged two-body B decays at LHCb
Public Note
2   Reconstruction and selection of $B \to h^+ h'^-$ **decays**

Ref: *CERN-LHCb-2007-059*
Issue: *1*
Date: *September 8, 2007*

2.2   Event selection

In order to optimize the selection and evaluate the yields and the background contamination, the following sources of background have been considered:

- specific background cross-feeds: every charmless charged two-body decay of the B_d, B_s and Λ_b is a potential source of background for the other modes in case of mis-identification ($\pi/K/p$).

- $b\bar{b}$-inclusive: it is expected as the dominant source of combinatorial background. This is due to the fact that the decay products of B-hadrons can better mimic particles from signal events.

The offline selection, as for all the other event selections in LHCb, has been realized in two separate steps. First, the so called pre-selection is performed, in order to reduce the $b\bar{b}$-inclusive combinatorial background by roughly a factor 10^3 by means of soft cuts, thus keeping a high efficiency on signal events. This step has the aim of reducing the size of the sample, allowing for a significant reduction of the computing power needed for the final optimization of the selection. In fact, the final selection performed on the pre-selected sample is basically a fine tuning of the previous step, where more sophisticated algorithms can be employed in order to identify the most convenient cuts that maximize the event yields and minimize the background contamination.

The optimization has been performed before any trigger algorithm is simulated. In fact, the general strategy in LHCb has consisted so far in optimizing the trigger algorithm on events useful for the offline analysis. For this reason it is usually applied once the offline selection is over, even if in the real world the opposite will obviously happen. In the following, any time a selection efficiency will be mentioned, it is intended to be relative to Monte Carlo generated events, while the trigger efficiency has to be understood as relative to offline selected events.

2.2.1   The pre-selection

The first step of the pre-selection consists in applying some filter criteria to each pair of oppositely charged tracks in the event:

- the impact parameter significances of the tracks, computed with respect to all the reconstructed primary vertices, must exceed a given threshold (i);

- the transverse momenta of the tracks must be greater than a given threshold (ii).

These two simple criteria provide a reduction of the initial sample. They reflect the basic signatures of the B-meson decays, i.e. the relatively long life (an average B-meson reconstructed at LHCb is expected to fly order of 1 cm before decaying), and the large mass of the decaying B, leading to a large transverse momentum of the daughters with respect to minimum bias and underlying event primary particles.

Then, for each pair of oppositely charged tracks it is required that:

- the invariant mass, calculated assuming for each track the pion hypothesis, must lie in a large window centered around the B mass region (iii);

- the transverse momentum of at least one of the two tracks must exceed a given threshold (iv);

- the maximum of the impact parameter significances of at least one of the two tracks, computed with respect to all the reconstructed primary vertices, must be larger than a given threshold (v).

Each pair surviving these cuts is then used to form the B-decay vertex by means of a common vertex fit, and then the momenta of the two tracks are summed up to form a B candidate. The B candidate is further requested to satisfy the following selection criteria:

Charmless charged two-body B decays at LHCb
Public Note
2   Reconstruction and selection of $B \to h^+ h'^-$ decays

Ref: *CERN-LHCb-2007-059*
Issue: *1*
Date: *September 8, 2007*

ID	Cut type	Accepted values
i	$min[(IP/\sigma_{IP})^h,\ (IP/\sigma_{IP})^{h'}]$	> 3.5
ii	$min(p_T^h,\ p_T^{h'})\ [GeV/c]$	> 0.6
iii	$m_{\pi\pi}\ [GeV/c^2]$	$[3.3 - 7.3]$
iv	$max(p_T^h,\ p_T^{h'})\ [GeV/c]$	> 2.0
v	$max[(IP/\sigma_{IP})^h,\ (IP/\sigma_{IP})^{h'}]$	> 5.5
vi	χ^2	< 6
vii	$p_{T_B}\ [GeV/c]$	> 0.7
viii	L_B/σ_{L_B}	> 12
ix	IP_B/σ_{IP_B}	< 3.15

Table 4 Summary of pre-selection cuts. The ID column refers to the labels used in the text.

Pre-selection	$B \to h^+ h'^-$	$b\bar{b}$-inclusive
Analyzed events	252000	27288409
Events after pre-selection	56233	23174
Reduction factor	4.5	1177

Table 5 Number of events surviving after the pre-selection cuts for signal and $b\bar{b}$-inclusive background. The reduction factors are also shown.

- the maximum value of the vertex fit χ^2 must not exceed a given limit (vi);

- the transverse momentum of the B candidate must be larger than a threshold (vii);

- the distance of flight, calculated as 3D distance between the primary and secondary vertices, must have a significance exceeding a threshold (viii);

- the direction of flight must point to the primary vertex; this is accomplished by a cut on the maximum value of the impact parameter significance of the B candidate (ix).

The values of the pre-selection cuts are summarized in Tab. 4. The distributions of all the selection variables, obtained before applying the pre-selection cuts for signal and $b\bar{b}$-inclusive events, are shown in Fig. 1.

The number of $B \to h^+ h'^-$ and $b\bar{b}$-inclusive events surviving the pre-selection cuts and the reduction factors are summarized in Tab. 5. The pre-selection cuts allow to reduce the combinatorial background from $b\bar{b}$-inclusive events by about a factor 1200, while the signal sample is reduced only by a factor 4.5.

2.2.2   *The selection*

The selection algorithm is completely analogous to the pre-selection one, but with tighter cuts and with the addition of particle identification criteria.

The particle identification procedure and calibration will be described in the next section. Here we just mention that, differently from the pre-selection, where just one algorithm existed since all the particles were given the pion hypothesis, in this case the particle identification introduces a distiction between the various channels. Hence we can speak of different selection algorithms[2].

Using the sample data filtered by the pre-selection algorithm, the final selection cuts - with the exception of the particle identification cuts which are treated separately - have been optimized by maximizing the ratio $S/\sqrt{S+B}$, where S stands for the number of signal events while B stands for the

---

[2]An alternative approach that makes no use of particle identification cuts at the selection level, but which aims to use full information embedded in the particle identification likelihood at a later phase, is under development. In this note we just describe the traditional approach of standard particle identification cuts at the event selection level.

Charmless charged two-body B decays at LHCb
Public Note
2   Reconstruction and selection of $B \to h^+ h'^-$ decays

Ref: *CERN-LHCb-2007-059*
Issue: *1*
Date: *September 8, 2007*
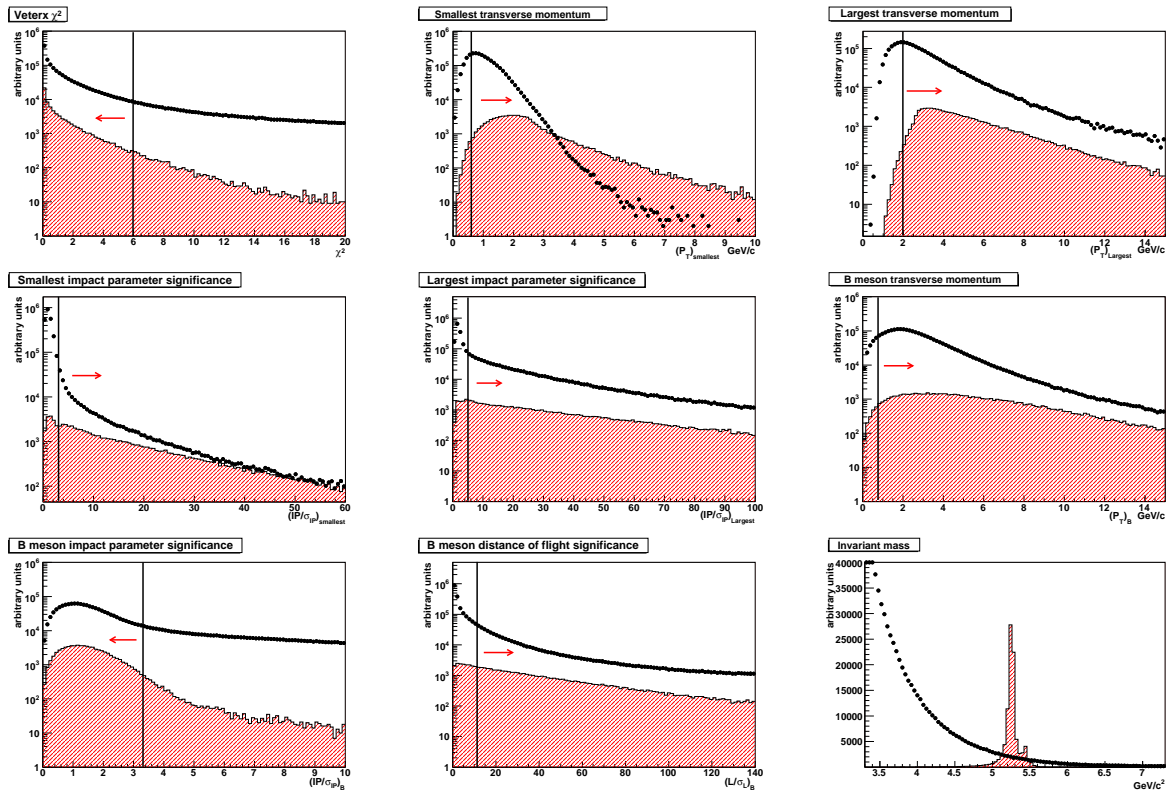
Figure 1 Distributions of all the pre-selection variables, before applying the pre-selection cuts, for true $B \to h^+ h'^-$ e $\Lambda_b \to p h^-$ events (clear histograms) and $b\bar{b}$-inclusive background (dark circles). The cut values are shown as vertical lines and the arrows indicate the regions accepted by the pre-selection.

Charmless charged two-body B decays at LHCb
Public Note
2 Reconstruction and selection of $B \to h^+h'^-$ decays

Ref: *CERN-LHCb-2007-059*
Issue: *1*
Date: *September 8, 2007*

ID	Cut type	Accepted values
i	$min[(IP/\sigma_{IP})^h, (IP/\sigma_{IP})^{h'}]$	> 6
ii	$min(p_T^h, p_T^{h'}) \, [GeV/c]$	> 1
iii	$|\Delta m| \, [GeV/c^2]$	< 0.05
iv	$max(p_T^h, p_T^{h'}) \, [GeV/c]$	> 3
v	$max[(IP/\sigma_{IP})^h, (IP/\sigma_{IP})^{h'}]$	> 12
vi	χ^2	< 5
vii	$p_{T_B} \, [GeV/c]$	> 1.2
viii	L_B/σ_{L_B}	> 18
ix	IP_B/σ_{IP_B}	< 2.5

Table 6 Summary of selection cuts, excluding particle identification ones. In order to apply the invariant mass cut around the nominal B-meson or Λ_b-baryon of interest, it is necessary to identify the daughter particles. The particle identification cuts are described in Section 2.3.

number of $b\bar{b}$-inclusive events. The optimization has been performed by varying all the cut values simultaneously over a fixed-step multi-dimensional lattice. The lattice had a dimension 9, according to the number of cuts to be optimized, with 5 grid points per dimension. Hence, the total number of combinations to be explored was $5^9 = 1953125$. In order not to be limited by a huge computation time, the lattice scan was parallelized over 125 CPUs, i.e. each of the 125 partitions was characterized by just $5^6 = 15625$ combinations. The optimal set of cuts was thus determined as the one corresponding to the maximum $S/\sqrt{S+B}$ value amongst the 125 determined maxima. We repeated the procedure several times with different cut ranges, in order to be confident to have not indentified a local minimum, and also checking that each best cut was not lying at any border of the lattice.

In order not to introduce systematic differences between the various $B \to h^+h'^-$ channels through the selection, a unique set of cuts has been chosen for all the decay modes.

Tab. 6 shows the final values of the selection cuts. In order to give an estimate of the background-to-signal ratios, an invariant mass cut around the nominal B-hadron mass of interest is applied for each different mass hypothesis of the daughter particles.

The results of the event selection are summarized in Tab. 7. The values correspond to the number of events surviving after the selection cuts for each $B \to h^+h'^-$ and $\Lambda_b \to ph^-$ decay. In order to increase the effective $b\bar{b}$-inclusive statistics, for a better evaluation of the background-to-signal ratio, a larger window for the invariant mass cut ($\Delta m = \pm 600 \, \text{MeV}/c^2$) has been used while running the selection over $b\bar{b}$-inclusive events. This was necessary since the number of $b\bar{b}$-inclusive events was statistically limited, and just a handful of events would have survived if a tight mass window was used, resulting in a problematic evaluation of the B/S. The mass window is 12 times larger than the one applied to signal events. Under the assumption that the mass distribution of $b\bar{b}$-inclusive events is approximately linear in such a window, we can effectively increase the $b\bar{b}$ statistics by a factor 12.

It is worth noting that background events in the right sideband of the mass spectrum with respect to the signal peak are expected to be of pure combinatorial origin, while those in the left sideband should be dominated by partially reconstructed specific B decays, such as $B \to \rho\pi$ or $B \to K^*\pi$, where one particle from the decays of the resonances is missed. The Monte Carlo $b\bar{b}$-inclusive statistics available for this study did not allow to make a comprehensive study of the nature of the combinatorial background. However we can consider the combinatorial background-to-signal ratios estimated this way as quite conservative.

The number of $b\bar{b}$-inclusive events selected (excluding signal events which are also present inside the $b\bar{b}$-inclusive sample) are shown in the last row of Tab. 7.

Charmless charged two-body B decays at LHCb
Public Note
2   Reconstruction and selection of $B \to h^+ h'^-$ decays

Ref: *CERN-LHCb-2007-059*
Issue: *1*
Date: *September 8, 2007*

MC sample	Selection algorithm					
	$B_d \to \pi^+\pi^-$	$B_d \to K^+\pi^-$	$B_s \to \pi^+ K^-$	$B_s \to K^+ K^-$	$\Lambda_b \to p\pi^-$	$\Lambda_b \to pK^-$
$B_d \to \pi^+\pi^-$	**3053**	173	73	2	1	0
$B_d \to K^+\pi^-$	211	**11543**	229	188	21	8
$B_s \to \pi^+ K^-$	8	13	**761**	25	2	0
$B_s \to K^+ K^-$	1	52	96	**2842**	1	17
$\Lambda_b \to p\pi^-$	1	5	6	0	**755**	16
$\Lambda_b \to pK^-$	2	6	9	14	55	**2722**
$b\bar{b}$-inclusive	34	40	35	1	30	2

Table 7   Number of signal and $b\bar{b}$-inclusive events surviving the selection algorithms. The rows of the matrix distinguish the various event samples, while the columns the selection algorithms. The selection algorithms share the same selection cuts, but differ for the particle identification.

2.3   Particle identification

The particle identification at LHCb is based on the information provided by the RICH system (12; 13), the electromagnetic and hadronic calorimeters (14), including pre-shower and scintillator pad detectors, and the muon chambers (15).

The variable used to discriminate between different particle hypotheses is $\Delta \log \mathcal{L}_{AB}$, which for each track is defined as:

$$\Delta \log \mathcal{L}_{AB} = \log \mathcal{L}_A - \log \mathcal{L}_B, \tag{1}$$

where $\mathcal{L}_A$ and $\mathcal{L}_B$ are the likelihoods for particle hypotheses A and B respectively.

In order to select the different decay modes $B \to h^+ h'^-$ and $\Lambda_b \to ph^-$, the following criteria are used:

- if $\Delta \log \mathcal{L}_{\mu\pi} > -8$ the track is a **muon**, otherwise it is **not a muon** and the next hypothesis is explored;

- if $\Delta \log \mathcal{L}_{e\pi} > 0$ the track is an **electron**, otherwise it is **not an electron** and the next hypothesis is explored;

- if $\Delta \log \mathcal{L}_{K\pi} > 2$ and $\Delta \log \mathcal{L}_{Kp} > -2$ the track is a **kaon**, otherwise it is **not a kaon** and the next hypothesis is explored;

- if $\Delta \log \mathcal{L}_{p\pi} > 3$ the track is a **proton**, otherwise it is **not an proton** and the next hypothesis is explored;

- if $\Delta \log \mathcal{L}_{K\pi} < -2$ the track is a **pion**, otherwise the track is **discarded**.

The capabilities of LHCb in separating pions from kaons are clearly visible in Fig. 2(a), which shows the $\Delta \log \mathcal{L}_{K\pi}$ distributions for true pions and kaons from $B \to h^+ h'^-$ decays. By cutting on this variable a clean separation of the various modes can be achieved. The invariant mass distributions in the $\pi^+\pi^-$ hypothesis are shown in Figg. 2(b) and 3 before and after the employment of the PID information. For each distribution the corresponding cross-feed background coming from all the other charmless charged two-body decays $B \to h^+ h'^-$ and $\Lambda_b \to ph^-$ is also shown.

The PID information will be calibrated on data using control samples. We have focused on the $D^* \to D^0\pi$ followed by $D^0 \to K\pi$ decay chain given its "golden kinematics" that allows the selection of very clean samples of charged kaons and pions without using the particle identification information, but with a purity close to 100%. A large sample of such D^* decays will be acquired with a dedicated trigger stream for which LHCb foresees a bandwidth to tape of about 300 Hz.

Charmless charged two-body B decays at LHCb
Public Note
2 Reconstruction and selection of $B \rightarrow h^+ h^{'-}$ decays

Ref: *CERN-LHCb-2007-059*
Issue: *1*
Date: *September 8, 2007*
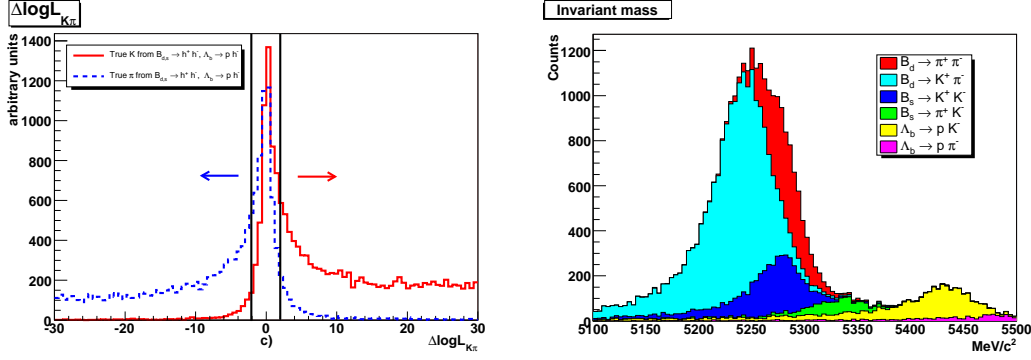
Figure 2 (a) Left: $\Delta \log \mathcal{L}_{K\pi}$ distribution for true kaons and pions from $B \rightarrow h^+ h^{'-}$ decays. The vertical line shows the applied cut. The blue arrow shows the acceptance region for the pions, while the red one for the kaons. (b) Right: Invariant mass distribution for the $B \rightarrow h^+ h^{'-}$ and $\Lambda_b \rightarrow ph^-$ signal events after the pre-selection. The invariant mass is computed under the $\pi^+\pi^-$ hypothesis.

The $\Delta log\mathcal{L}_{K\pi}$ distributions for pions and kaons selected from the control sample, and from $B \rightarrow h^+ h^{'-}$ decays after the event selection, where the Monte Carlo truth information has been used to identify the daughter particles, are quite different in general, as shown in Fig. 4. This is particularly true for values of the $\Delta log\mathcal{L}_{K\pi}$ around zero, i.e. in the region where the π/K discrimination power is weak. Such difference is not surprising, since the momentum spectra predicted by the simulation differ as well, as shown in Fig. 5. In fact, the RICH PID starts to be inefficient in the regions of large momenta, i.e. around 80-100 GeV/c or more, and of small momenta, around 5-10 GeV/c or less, while the average efficiency is large and has roughly a constant behaviour in the intermediate range (13; 16).

As an example of how to correct for such differences, we can build the $\Delta log\mathcal{L}_{K\pi}$ distributions in bins of momentum. In Fig. 6 a comparison of the $\Delta log\mathcal{L}_{K\pi}$ distributions for the two samples in one bin of momentum 20 $GeV/c < p < 30$ GeV/c is shown. As it can be seen, the distributions agree pretty well in this case, even if the statistics used for this example is quite limited. At present we are waiting for the mass production of much larger Monte Carlo samples of D^* decays which will allow a comprehensive study of the PID calibration.

2.4 Efficiencies, yields and B/S evaluation

The total signal efficiency ϵ_{tot} can be factorized as:

$$\epsilon_{tot} = \epsilon_{gen} \times \epsilon_{sel/gen} \times \epsilon_{trig/sel} \tag{2}$$

where:

- ϵ_{gen} is the generation efficiency, taking into account the 400 mrad forward cut on the value of the production polar angle of the b-hadron coming from the primary collision;

- $\epsilon_{sel/gen}$ is the selection efficiency defined as the fraction of selected events with respect to generated events;

- $\epsilon_{trg/sel}$ is the trigger efficiency, defined as the fraction of events which pass the trigger with respect to the selected events.

The ϵ_{gen} values, $\epsilon_{sel/gen}$ and $\epsilon_{trg/sel}$ resulting from the simulation, the offline selection and the application of the trigger algorithm are reported in the Tab. 9. The annual signal yields can be computed as:

Charmless charged two-body B decays at LHCb
Public Note
2   Reconstruction and selection of $B \to h^+h'^-$ decays

Ref: *CERN-LHCb-2007-059*
Issue: *1*
Date: *September 8, 2007*
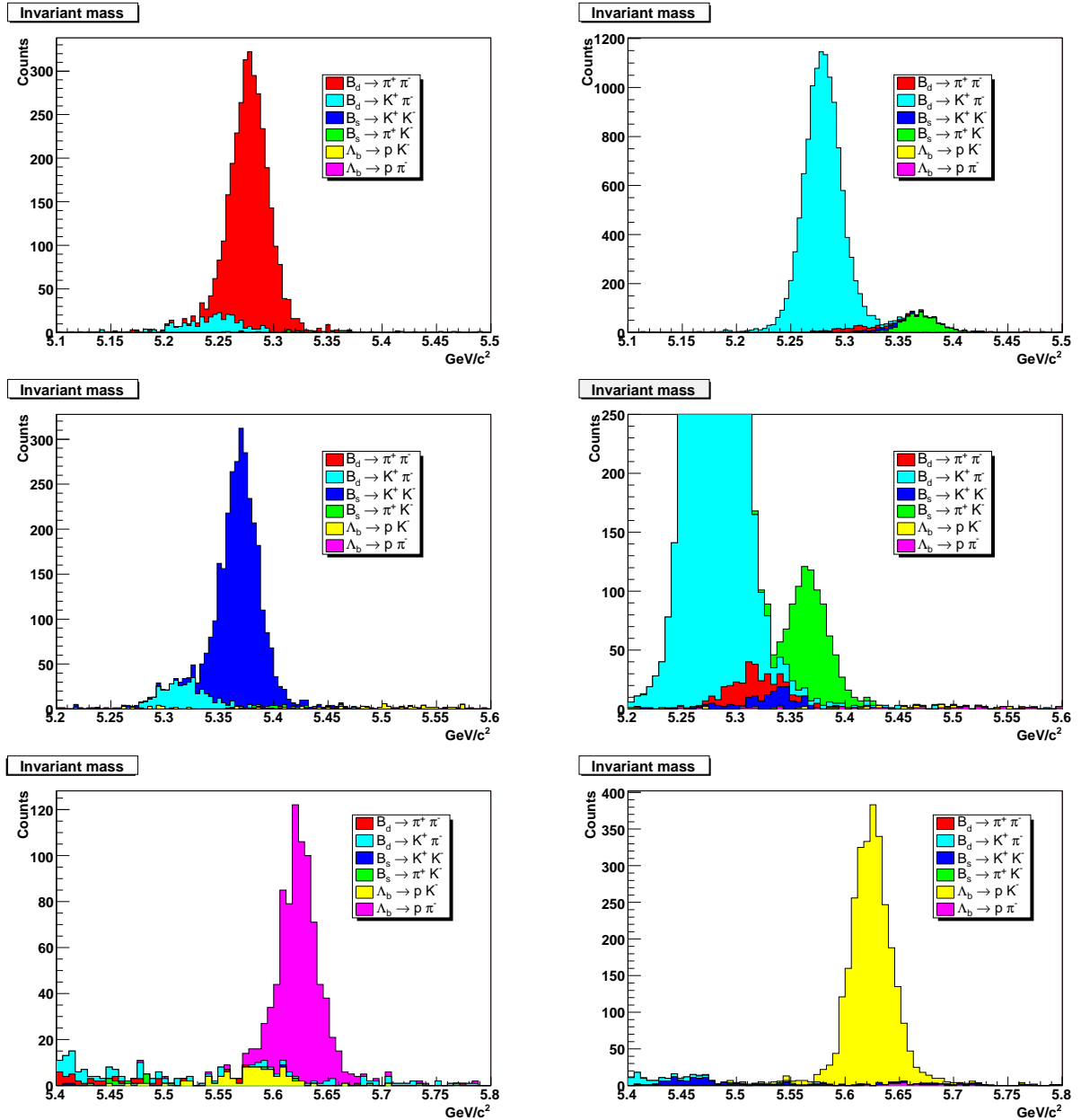
Figure 3 Invariant mass distributions for signal events $B \to h^+h'^-$ and $\Lambda_b \to ph^-$ after the selection and particle identification cuts. The great hadron PID potential of LHCb is clearly visible.

Charmless charged two-body B decays at LHCb
Public Note
2   Reconstruction and selection of $B \to h^+ h'^-$ **decays**

Ref: *CERN-LHCb-2007-059*
Issue: *1*
Date: *September 8, 2007*
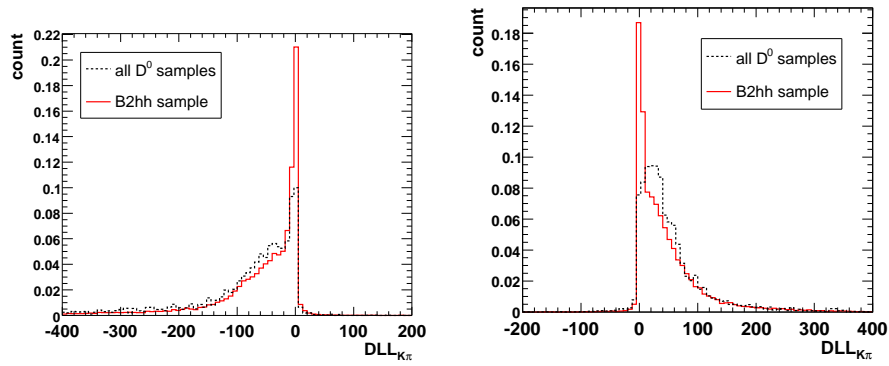
Figure 4 $\Delta log\mathcal{L}_{K\pi}$ distributions for pions (left) and kaons (right) selected from the $D^0 \to K\pi$ decay and from $B \to h^+ h'^-$ samples.
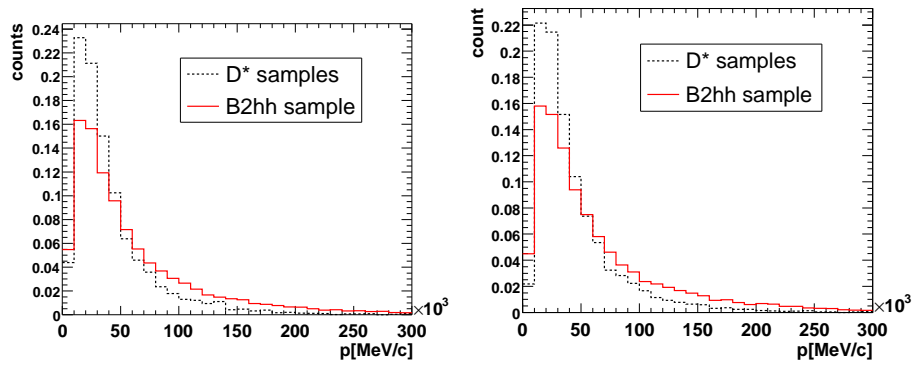
Figure 5 Momentum spectra for pions (left) and kaons (right) from $D^0 \to K\pi$ and $B \to h^+ h'^-$ samples.
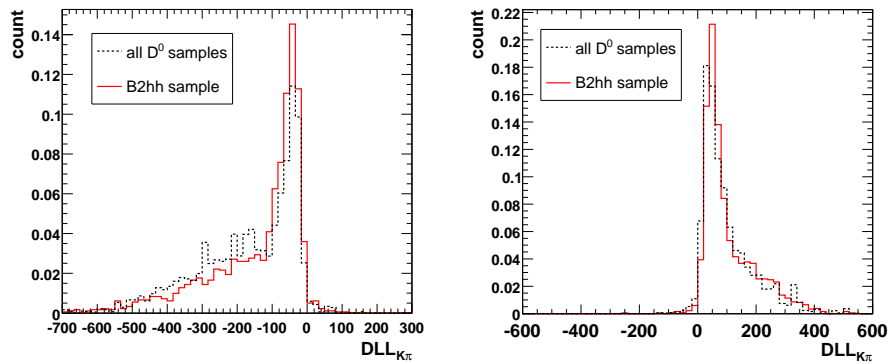
Figure 6 $\Delta log\mathcal{L}_{K\pi}$ distributions for pions (left) and kaons (right) from the $D^0 \to K\pi$ decay and from $B \to h^+ h'^-$ samples requiring $20\ GeV/c < p < 30\ GeV/c$.

$$S = \mathcal{L}_{LHCb} \times t_{year} \times \sigma_{b\bar{b}} \times 2 \times f_B \times \mathcal{BR} \times \epsilon_{tot}, \tag{3}$$

Charmless charged two-body B decays at LHCb   Ref: *CERN-LHCb-2007-059*
Public Note   Issue: *1*
2   Reconstruction and selection of $B \to h^+ h'^-$ decays   Date: *September 8, 2007*

Channel	Factor in (%) of $\epsilon_{tot}(\%)$			
	$\epsilon_{tot} = \epsilon_{gen} \times \epsilon_{sel/gen} \times \epsilon_{trg/sel}$			
	ϵ_{gen}	$\epsilon_{sel/gen}$	$\epsilon_{trg/sel}$	ϵ_{tot}
$B_d \to \pi^+\pi^-$	34.9 ± 0.3	7.36 ± 0.13	36.3 ± 1.1	0.93 ± 0.03
$B_d \to K^+\pi^-$	34.9 ± 0.3	7.21 ± 0.07	36.8 ± 0.6	0.93 ± 0.02
$B_s \to \pi^+K^-$	34.8 ± 0.3	7.25 ± 0.30	40.6 ± 2.3	1.02 ± 0.06
$B_s \to K^+K^-$	34.8 ± 0.3	7.11 ± 0.13	39.3 ± 1.2	0.97 ± 0.03
$\Lambda_b \to p\pi^-$	34.6 ± 0.3	7.20 ± 0.26	38.3 ± 2.3	0.95 ± 0.06
$\Lambda_b \to pK^-$	34.6 ± 0.3	6.80 ± 0.13	36.0 ± 1.1	0.86 ± 0.03

Table 8 Summary of efficiencies for the decays $B \to h^+ h'^-$ and $\Lambda_b \to ph^-$.

where f_B is the hadronization probability of the B-meson of interest (see Tab. 2), the factor 2 takes into account the production of two b-hadrons per event, $\mathcal{BR}$ is the branching ratio of the B decay under study, $\mathcal{L}_{LHCb} = 2 \cdot 10^{32}\ cm^{-2}s^{-1}$ is the average luminosity at the LHCb interaction point, $t_{year} = 10^7$ s is the amount of time assumed to correspond to one year of data taking and $\sigma_{b\bar{b}} = 500\ \mu$b is the $b\bar{b}$ production cross-section expected at $14\ TeV$.

The combinatorial $b\bar{b}$-inclusive background-to-signal ratio is given by:

$$\left(\frac{B}{S}\right)^{b\bar{b}} = \frac{\epsilon_{gen}^{b\bar{b}} \cdot \epsilon_{sel/gen}^{b\bar{b}}}{2 \cdot f_B \cdot \mathcal{BR} \cdot \epsilon_{gen}^{sig} \cdot \epsilon_{sel/gen}^{sig}}, \tag{4}$$

where $\epsilon_{gen}^{b\bar{b}}$ and ϵ_{gen}^{sig} are the generation efficiencies for $b\bar{b}$-inclusive and signal events respectively, while $\epsilon_{sel/gen}^{b\bar{b}}$ and $\epsilon_{sel/gen}^{sig}$ are the corresponding selection efficiencies.

As is evident in Eq. 4, we are not taking into account the trigger. This is done in order to increase the $b\bar{b}$-inclusive effective statistics. It corresponds to assuming that the trigger efficiencies on $b\bar{b}$-inclusive and signal selected events are approximately identical, which is a good approximation since the offline selection is so tight to let only events which have a signature very similar to the signal survive. With the same aim, as already mentioned, the selection of $b\bar{b}$-inclusive events has been performed using a large mass window, $\pm 600\ \mathrm{MeV}/c^2$, around the nominal B-meson mass.

Finally, the specific cross-feed backgrounds coming from all the other charmless charged two-body decays for each signal under consideration, can be estimated by:

$$\left(\frac{B}{S}\right)^{spec} = \frac{\sum_j f_B^j \cdot \mathcal{BR}^j \cdot \epsilon_{gen}^j \cdot \epsilon_{sel/gen}^j}{f_B^{sig} \cdot \mathcal{BR}^{sig} \cdot \epsilon_{gen}^{sig} \cdot \epsilon_{sel/gen}^{sig}}, \tag{5}$$

where the superscript "sig" indicates the signal and the sum index runs over all the other channels, $B \to h^+ h'^-$ and $\Lambda_b \to ph^-$, excluding the signal under study. The ϵ_{gen} and $\epsilon_{sel/gen}$ values used to compute B/S are taken from Tab. 8.

Tab. 8 summarizes the signal efficiencies, while Tab. 9 the untagged annual yield and the B/S ratios from specific and $b\bar{b}$-inclusive backgrounds for all the $B \to h^+ h'^-$ and $\Lambda_b \to ph^-$ decays.

2.5   Mass resolution

In a two-body decay the invariant mass squared can be expressed as follows:

$$m^2 = (p_1 + p_2)^2 = p_1^2 + p_2^2 + 2p_1 \cdot p_2 = m_1^2 + m_2^2 + 2(E_1 E_2 - p_1 p_2 \cos\theta), \tag{6}$$

Charmless charged two-body B decays at LHCb
Public Note
2   Reconstruction and selection of $B \to h^+ h'^-$ decays

Ref: *CERN-LHCb-2007-059*
Issue: *1*
Date: *September 8, 2007*

Channel	Annual yield $L = 2 fb^{-1}$	B/S from $b\bar{b}$-inclusive background	B/S from specific background
$B_d \to \pi^+ \pi^-$	35700	0.5	0.07
$B_d \to K^+ \pi^-$	137600	0.15	0.02
$B_s \to \pi^+ K^-$	9800	1.9	0.5
$B_s \to K^+ K^-$	35900	< 0.06	0.07
$\Lambda_b \to p\pi^-$	9100	1.7	0.1
$\Lambda_b \to pK^-$	31800	< 0.08	0.02

Table 9 Untagged annual yields and background-to-signal ratios from specific and $b\bar{b}$-inclusive backgrounds, for the decays $B \to h^+ h'^-$ and $\Lambda_b \to ph^-$.
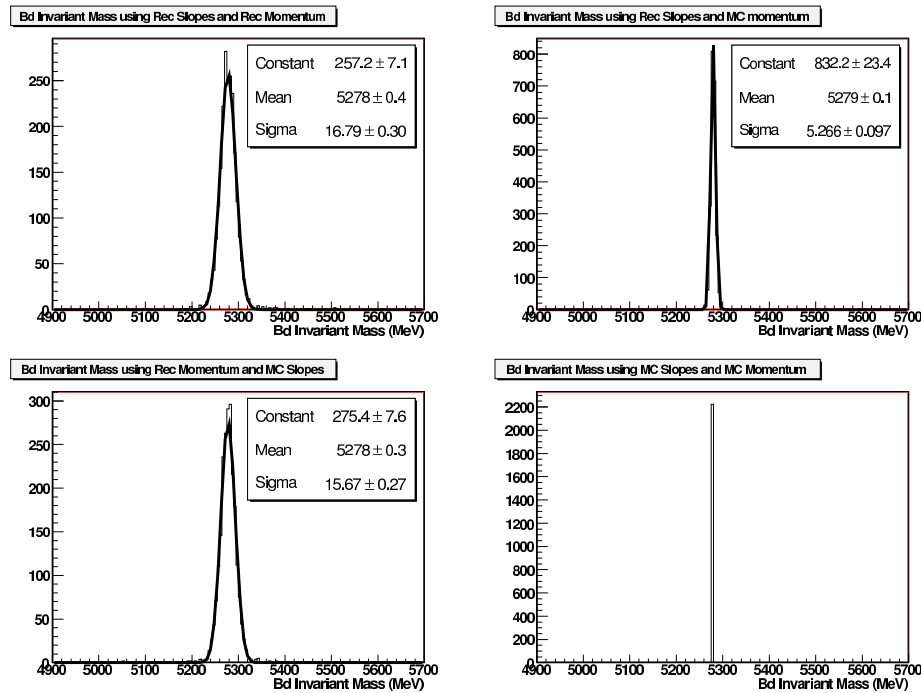
Figure 7 The B_d mass distribution obtained using in Eq. 6: the reconstructed momentum and the reconstructed angle θ (Top left), the Monte Carlo true momentum and the reconstructed angle θ (Top right), the reconstructed momentum and the Monte Carlo true angle θ (Bottom left), the Monte Carlo true momentum and true angle θ (Bottom right).

where m_1, m_2, E_1, E_2, p_1 and p_2 are the masses, the energies and the momenta of the first and of the second decay products, while θ is the polar angle between the directions of the two momenta. Assuming $E \approx p$, Eq. 6 becomes:

$$m^2 \approx m_1^2 + m_2^2 + 2p_1 p_2 (1 - \cos\theta) \tag{7}$$

and the uncertainty on the invariant mass (δm) can be obtained as:

$$(\delta m)^2 = \frac{[p_1 p_2 (1 - \cos\theta)]^2}{m^2} \left[\left(\frac{\delta p_1}{p_1}\right)^2 + \left(\frac{\delta p_2}{p_2}\right)^2 + \frac{\sin^2\theta}{(1 - \cos\theta)^2} (\delta\theta)^2 \right], \tag{8}$$

In Fig. 7 the effect of the various uncertainties contributing to the invariant mass resolution are shown,

Charmless charged two-body B decays at LHCb
Public Note
2   Reconstruction and selection of $B \to h^+ h'^-$ decays

Ref: *CERN-LHCb-2007-059*
Issue: *1*
Date: *September 8, 2007*

for events selected as discussed in Sec. 2.2. The figure illustrates that δm is dominated by the momentum resolution[3] of the two daughters.

Several sources of uncertainties affect the measurement of the momentum of the decay products. Studies reported in (17; 18) show the effects of misalignments of the Outer Tracker (19) on the momentum resolution and in general on the tracking performance. These studies show that in the worst case scenario the momentum resolution deteriorates from the nominal value of approximately 0.4% to a maximum value of approximately 0.8%. In the following the net effect of the deteriorated momentum resolution on the invariant mass will be simply illustrated with the help of a toy Monte Carlo.

In order to obtain different values of the momentum uncertainty the value of the reconstructed momentum has been smeared with a Gaussian distribution, centered on p_{rec} and with a σ which can be varied. The results obtained for the $B_d \to \pi^+ \pi^-$ are shown in Fig. 8. The net effect of worsening the momentum resolution from the nominal value of approximately 0.4% to approximately 0.7% both for the π^+ and for the π^- causes a degradation of the invariant mass resolution from approximately 17 MeV/c^2 to 29 MeV/c^2.
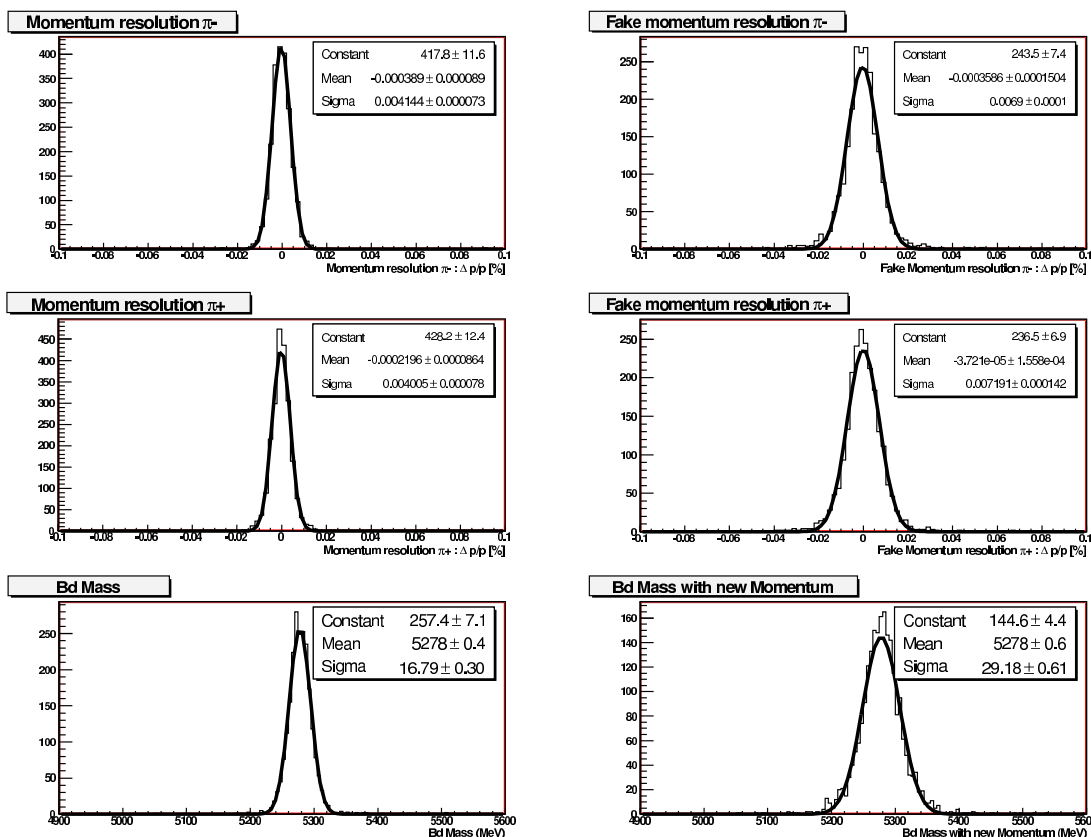
Figure 8 (Left): From top to bottom, the momentum resolution of the π^-, the momentum resolution of the π^+ and the B_d mass distribution. (Right): From top to bottom, the smeared momentum resolution of the π^-, the smeared momentum resolution of the π^+ and the corresponding B_d mass distribution.

This procedure has been iterated for several values of the momentum resolution and the results are

---

[3]The momentum resolution is defined as $\frac{\Delta p}{p} = \frac{p_{rec} - p_{MC}}{p_{MC}}$, where p_{rec} is the reconstructed momentum as obtained from the track-fitting and p_{MC} is the Monte Carlo momentum.

Charmless charged two-body B decays at LHCb
Public Note
2   Reconstruction and selection of $B \to h^+ h'^-$ decays

Ref: *CERN-LHCb-2007-059*
Issue: *1*
Date: *September 8, 2007*

summarized in Fig. 9 for the $B_d \to \pi^+ \pi^-$[4].
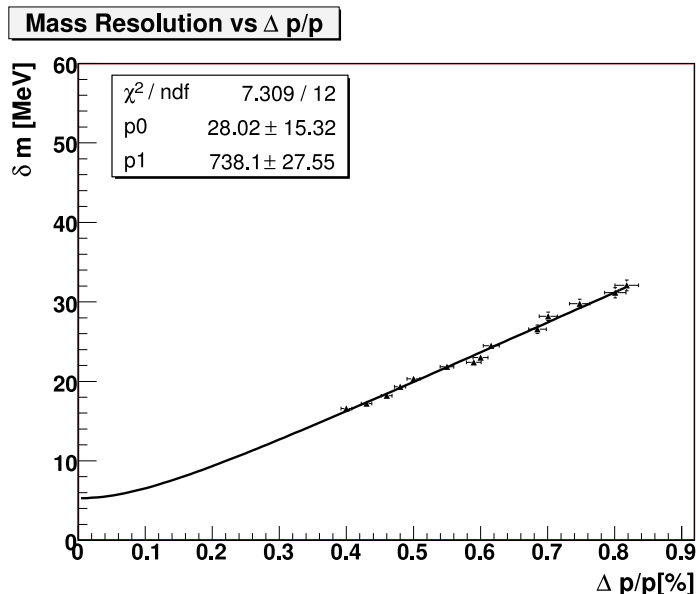
Figure 9 The B_d invariant mass resolution as a function of the momentum resolution. The fit to the data using Eq. 9 is superimposed.

In Fig. 9 the mass resolution is plotted as a function of the momentum resolution. The momentum resolution values vary from the nominal 0.4% value to a maximum of approximately 0.8%. The Eq. 8, approximated by the following form:

$$(\delta m) = \sqrt{\left[p1 \left(\frac{\delta p}{p} \right)^2 + (p0) \right]}, \tag{9}$$

has been used to fit the data. The result is shown in Fig. 9. Notice that the angular resolution extrapolated from the fit to the data in Fig. 9 corresponds to the one shown in Fig. 7 (top-right).

This study has been repeated for all the four $B \to h^+ h^-$ channels and the results obtained are similar. Large differences between the various channels arise however when the different backgrounds are taken into account.

Misalignments of the tracking system deteriorating the momentum resolution and thus the invariant mass resolution will obviously affect the background-to-signal ratios. The amount of combinatorial background, at fixed signal yields, will scale linearly with the mass resolution. In the following we will study the variation of the B/S ratio for the specific backgrounds, i.e. due to cross-feeds from the other $B \to h^+ h^-$ channels in case of particle misidentifications, as function of the mass resolution. The situation is particularly critical for the $B_s \to \pi^+ K^-$ decay, which is characterized by a small branching fraction and cannot be separated from the much more abundant $\bar{B}_d \to \pi^+ K^-$ decay by the particle identification system. In Fig. 10 (left) the $B_s \to \pi^+ K^-$ signal peak and the $\bar{B}_d \to \pi^+ K^-$ background only, situated at the left of the signal peak, are shown.

The procedure of degrading the momentum resolution of both the $B_s \to \pi^+ K^-$ and the $\bar{B}_d \to \pi^+ K^-$ events determines what is shown in Fig. 10 (center) and Fig. 10 (right). In Fig. 10 (center) the momentum resolution considered is approximately 0.5%; a larger number of background events belonging to the $\bar{B}_d \to \pi^+ K^-$ peak fall into the 100 MeV mass window, while in Fig. 10 (right) the momentum resolution is approximately 0.75% and the $\bar{B}_d \to \pi^+ K^-$ background strongly dominates the $B_s \to \pi^+ K^-$ signal.

---

[4]Similar plots have been obtained for all the decays of interest.

Charmless charged two-body B decays at LHCb
Public Note
2   Reconstruction and selection of $B \to h^+ h'^-$ **decays**

Ref: *CERN-LHCb-2007-059*
Issue: *1*
Date: *September 8, 2007*
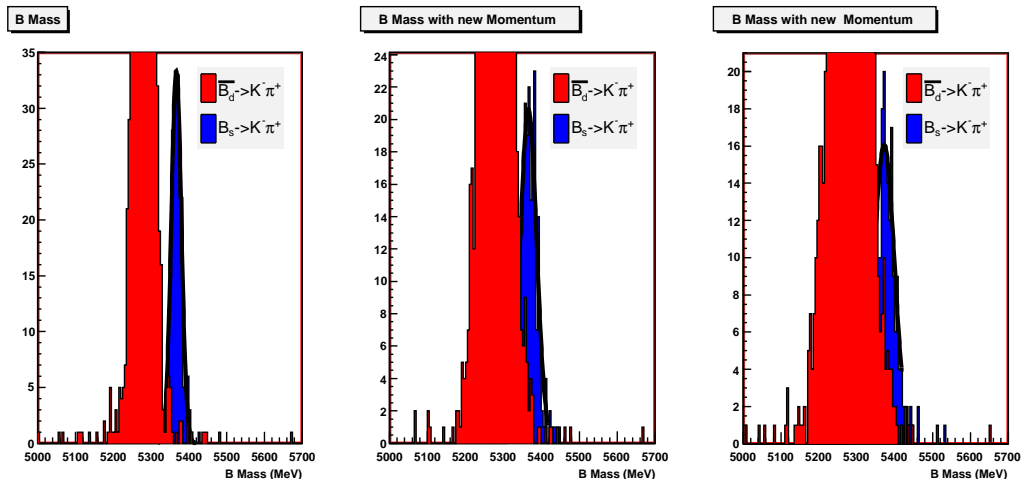
Figure 10 (Left): Mass separation between the signal decay $B_s \to \pi^+ K^-$ and the background decay $\bar{B}_d \to \pi^+ K^-$. (Center): The effect of smearing the momentum and degrading the mass resolution of the $B_s \to \pi^+ K^-$ and of the $\bar{B}_d \to \pi^+ K^-$ for a value of momentum resolution of approximately 0.5%. (Right): The effect of smearing the momentum and degrading the mass resolution of the $B_s \to \pi^+ K^-$ and of the $\bar{B}_d \to \pi^+ K^-$ for a value of momentum resolution of approximately 0.75%.

In Fig. 11 the B/S ratio is plotted as a function of the B_s mass resolution. After applying the smearing, the mass window cut of 100 MeV is applied. The five values of mass resolution adopted correspond approximately to the following values of momentum resolutions, 0.4%, 0.5%, 0.6%, 0.7% and 0.8%.
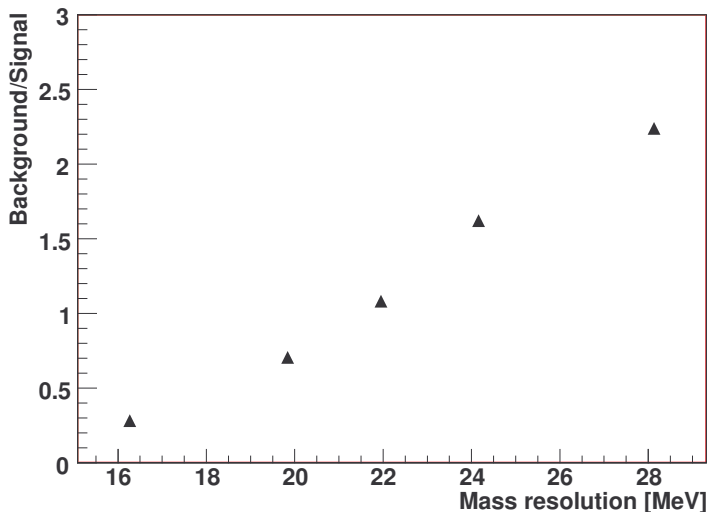
Figure 11 The B/S ratio as a function of the B_s mass resolution for the $B_s \to \pi^+ K^-$; the background considered is the $\bar{B}_d \to \pi^+ K^-$. The mass window used is 100 MeV.

The $B_d \to \pi^+ \pi^-$, the $B_d \to K^+ \pi^-$ and the $B_s \to K^+ K^-$ decays do not suffer a clear degradation of the specific B/S ratio, unlike the $B_s \to \pi^+ K^-$ decay. In these cases the procedure of smearing the momentum of both the signal and the background events leaves the B/S ratio constant since both some signal events and some background events do not fall inside the 100 MeV mass window. The

Charmless charged two-body B decays at LHCb
Public Note
3   CP violation studies

Ref: *CERN-LHCb-2007-059*
Issue: *1*
Date: *September 8, 2007*

results for the $B_d \to \pi^+\pi^-$, the $B_d \to K^+\pi^-$ and $B_s \to K^+K^-$ are summarized in Table 10.

Channel of interest					
$B_d \to \pi^+\pi^-$		$B_d \to K^+\pi^-$		$B_s \to K^+K^-$	
Mass Resolution (MeV)	B/S	Mass Resolution (MeV)	B/S	Mass Resolution (MeV)	B/S
16.7 ± 0.3	0.07	16.6 ± 0.3	0.02	16.1 ± 0.2	0.07
19.9 ± 0.4	0.07	19.5 ± 0.3	0.02	19.3 ± 0.3	0.07
23.2 ± 0.5	0.07	22.1 ± 0.3	0.02	22.2 ± 0.5	0.07
26.8 ± 0.8	0.07	26.9 ± 0.6	0.02	26.5 ± 0.7	0.07
29.9 ± 1.1	0.07	29.8 ± 0.8	0.02	29.3 ± 0.8	0.07

Table 10 Summary of variations of the B/S ratios as a function of the mass resolution for the $B_d \to \pi^+\pi^-$, the $B_d \to K^+\pi^-$ and $B_s \to K^+K^-$; the background considered is the $B_d \to K^+\pi^-$ for the $B_d \to \pi^+\pi^-$ and for the $B_s \to K^+K^-$, while is the $B_d \to \pi^+\pi^-$ for the $B_d \to K^+\pi^-$.

These studies show that a possible degradation of the momentum resolution from its nominal value of 0.4% might lead to increasing difficulty in observing clearly the $B_s \to \pi^+K^-$ decay.

3   CP violation studies

The main interest in collecting large samples of charmless B decays consists in measuring with high precision CP violation, which may reveal inconsistencies with the Standard Model predictions, i.e. sizeable effects of New Physics due to the presence of non-negligible penguin contributions to the amplitudes. In particular, as we will see in the final part of this paper, CP asymmetries measured with these channels can be used to constrain the U-spin flavour symmetry and/or to extract the γ angle of the Unitarity Triangle. In this section we review the formalism needed to deal with charmless charged two-body B decays, and describe the likelihood fit used to extract the CP parameters from the sample of selected B candidates. Finally, we present the expected sensitivites that can be reached with an integrated luminosity of 2 fb^{-1}, corresponding to one nominal year of LHCb data taking.

3.1   CP formalism and theoretical decay rates

The decay rates for initial neutral B and $\overline{B}$ mesons, decaying into a final state f at generic proper time t, can be written as:

$$\Gamma_{B \to f}(t) = \frac{|A_f|^2}{2} e^{-\Gamma t} \left[I_+(t) + I_-(t) \right] \tag{10}$$

and

$$\Gamma_{\overline{B} \to f}(t) = \frac{|A_f|^2}{2} \left| \frac{p}{q} \right|^2 e^{-\Gamma t} \left[I_+(t) - I_-(t) \right]. \tag{11}$$

Analogously, for the CP-conjugated final state $\overline{f}$, one has:

$$\Gamma_{\overline{B} \to \overline{f}}(t) = \frac{\left| \overline{A}_{\overline{f}} \right|^2}{2} e^{-\Gamma t} \left[\overline{I}_+(t) + \overline{I}_-(t) \right] \tag{12}$$

Charmless charged two-body B decays at LHCb
Public Note
3   CP violation studies

Ref: *CERN-LHCb-2007-059*
Issue: *1*
Date: *September 8, 2007*

and

$$\Gamma_{\overline{B}\to\overline{f}}(t) = \frac{\left|\overline{A}_{\overline{f}}\right|^2}{2} \left|\frac{q}{p}\right|^2 e^{-\Gamma t} \left[\overline{I}_+(t) - \overline{I}_-(t)\right]. \tag{13}$$

A_f and $\overline{A}_{\overline{f}}$ are the instantaneous decay amplitudes for $B \to f$ and $\overline{B} \to \overline{f}$ respectively, and Γ is the average decay width for the two mass eigenstates $|B_L\rangle$ and $|B_H\rangle$, L and H denoting the lightest and the heaviest of the two states respectively.

The functions $I_+(t)$, $I_-(t)$, $\overline{I}_+(t)$ and $\overline{I}_-(t)$ are:

$$I_+(t) = \left(1 + |\lambda_f|^2\right) \cosh\frac{\Delta\Gamma}{2}t - 2Re(\lambda_f)\sinh\frac{\Delta\Gamma}{2}t, \tag{14}$$

$$I_-(t) = \left(1 - |\lambda_f|^2\right)\cos\Delta m\,t - 2Im(\lambda_f)\sin\Delta m\,t, \tag{15}$$

$$\overline{I}_+(t) = \left(1 + \left|\overline{\lambda}_{\overline{f}}\right|^2\right)\cosh\frac{\Delta\Gamma}{2}t - 2Re(\overline{\lambda}_{\overline{f}})\sinh\frac{\Delta\Gamma}{2}t \tag{16}$$

and

$$\overline{I}_-(t) = \left(1 - \left|\overline{\lambda}_{\overline{f}}\right|^2\right)\cos\Delta m\,t - 2Im(\overline{\lambda}_{\overline{f}})\sin\Delta m\,t, \tag{17}$$

where Δm is the mass difference, positive by definition:

$$\Delta m = m_H - m_L.$$

while $\Delta\Gamma$ is the difference of the decay widths of the mass eigenstates, whose sign is predicted to be positive in the SM:

$$\Delta\Gamma = \Gamma_L - \Gamma_H,$$

The complex numbers λ_f and $\overline{\lambda}_{\overline{f}}$ are defined by the following equations:

$$\lambda_f = \frac{q}{p}\frac{\overline{A}_f}{A_f} \tag{18}$$

and

$$\bar{\lambda}_{\overline{f}} = \frac{p}{q}\frac{A_{\overline{f}}}{\overline{A}_{\overline{f}}}. \tag{19}$$

If f is a CP eigenstate, one has $f = \overline{f}$, and the four decay rates reduce to two. We can define the time dependent CP asymmetry as:

$$\mathcal{A}_f^{CP}(t) = \frac{\Gamma_{\overline{B}\to f}(t) - \Gamma_{B\to f}(t)}{\Gamma_{\overline{B}\to f}(t) + \Gamma_{B\to f}(t)} = \frac{\left(|\lambda_f|^2 - 1\right)\cos\Delta m\,t + 2Im\lambda_f\sin\Delta m\,t}{\left(|\lambda_f|^2 + 1\right)\cosh\frac{\Delta\Gamma}{2}t - 2Re\lambda_f\sinh\frac{\Delta\Gamma}{2}t}, \tag{20}$$

In the derivation of 20 we have used $\left|\frac{q}{p}\right| \simeq 1$, that is a very good approximation for both the $B_d - \overline{B}_d$ and $B_s - \overline{B}_s$ systems (20). The weak phase q/p can be expressed as:

Charmless charged two-body B decays at LHCb
Public Note
3   CP violation studies

Ref: CERN-LHCb-2007-059
Issue: 1
Date: September 8, 2007

$$\frac{q}{p} = \begin{cases} \exp(-i\phi_d) = \exp(-2i\beta) & (B_d - \overline{B}_d \text{ mixing}) \\ \exp(-i\phi_s) = \exp(2i\beta_s) & (B_s - \overline{B}_s \text{ mixing}), \end{cases} \tag{21}$$

where β and β_s are the mixing angles of the B_d and B_s systems respectively.

Introducing the quantities

$$\mathcal{A}_f^{dir} = \frac{|\lambda_f|^2 - 1}{|\lambda_f|^2 + 1}, \tag{22}$$

$$\mathcal{A}_f^{mix} = \frac{2\mathrm{Im}\lambda_f}{|\lambda_f|^2 + 1} \tag{23}$$

and

$$\mathcal{A}_f^{\Delta} = \frac{2\mathrm{Re}\lambda_f}{|\lambda_f|^2 + 1}, \tag{24}$$

the time-dependent CP asymmetry 20 can be rewritten as

$$\mathcal{A}_f^{CP}(t) = \frac{\mathcal{A}_f^{dir} \cos \Delta m\, t + \mathcal{A}_f^{mix} \sin \Delta m\, t}{\cosh \frac{\Delta\Gamma}{2} t - \mathcal{A}_f^{\Delta} \sinh \frac{\Delta\Gamma}{2} t}. \tag{25}$$

$\mathcal{A}_f^{dir}$, $\mathcal{A}_f^{mix}$ and $\mathcal{A}_f^{\Delta}$ are by definition related by the following equation:

$$\left(\mathcal{A}_f^{dir}\right)^2 + \left(\mathcal{A}_f^{mix}\right)^2 + \left(\mathcal{A}_f^{\Delta}\right)^2 = 1. \tag{26}$$

The quantities $\mathcal{A}_f^{dir}$ and $\mathcal{A}_f^{mix}$ parametrize direct and mixing-induced CP violation respectively.

Another interesting case is when f is a flavor specific final state, i.e. $f \neq \overline{f}$. One can write:

$$\lambda_f = \overline{\lambda}_{\overline{f}} = 0, \tag{27}$$

since only the B has instantaneous access to the decay channel f, while only the $\overline{B}$ has instantaneous access to the decay channel $\overline{f}$. In this case, the functions $I_+(t)$, $I_-(t)$, $\overline{I}_+(t)$ and $\overline{I}_-(t)$ reduce to:

$$I_+(t) = \overline{I}_+(t) = \cosh \frac{\Delta\Gamma}{2} t \tag{28}$$

and

$$I_-(t) = \overline{I}_-(t) = \cos \Delta m\, t. \tag{29}$$

By using the four decay rates, one can define the following two decay asymmetries:

$$\mathcal{A}_f(t) = \frac{\Gamma_{\overline{B} \to f}(t) - \Gamma_{B \to f}(t)}{\Gamma_{\overline{B} \to f}(t) + \Gamma_{B \to f}(t)} = -\frac{\cos \Delta m\, t}{\cosh \frac{\Delta\Gamma}{2} t} \tag{30}$$

and

$$\mathcal{A}_{\overline{f}}(t) = \frac{\Gamma_{\overline{B} \to \overline{f}}(t) - \Gamma_{B \to \overline{f}}(t)}{\Gamma_{\overline{B} \to \overline{f}}(t) + \Gamma_{B \to \overline{f}}(t)} = \frac{\cos \Delta m\, t}{\cosh \frac{\Delta\Gamma}{2} t} \tag{31}$$

It is also possible to define the following CP asymmetry:

Charmless charged two-body B decays at LHCb
Public Note
3 CP violation studies

Ref: *CERN-LHCb-2007-059*
Issue: *1*
Date: *September 8, 2007*

$$\mathcal{A}_{f,\overline{f}}^{CP}(t) = \frac{\left[\Gamma_{\overline{B}\to\overline{f}}(t) + \Gamma_{B\to\overline{f}}(t)\right] - \left[\Gamma_{\overline{B}\to f}(t) + \Gamma_{B\to f}(t)\right]}{\left[\Gamma_{\overline{B}\to\overline{f}}(t) + \Gamma_{B\to\overline{f}}(t)\right] + \left[\Gamma_{\overline{B}\to f}(t) + \Gamma_{B\to f}(t)\right]},\tag{32}$$

that results to be not dependent on time, and identically equal to the charge asymmetry defined as:

$$\mathcal{A}_{f,\overline{f}} = -\frac{|A_f|^2 - \left|\overline{A}_{\overline{f}}\right|^2}{|A_f|^2 + \left|\overline{A}_{\overline{f}}\right|^2} = -\frac{1 - \left|\frac{\overline{A}_{\overline{f}}}{A_f}\right|^2}{1 + \left|\frac{\overline{A}_{\overline{f}}}{A_f}\right|^2}.\tag{33}$$

The charge asymmetry differs from zero in the presence of direct CP violation, and parametrizes it.

3.2 Experimental decay rates

In section 3.1 we have introduced the theoretical expressions of the decay rates for B and $\overline{B}$ decays. From an experimental point of view these expressions need to be modified, by taking into account the possibility of wrong tagging, the presence of background, the acceptance as a function of the proper time, the resolution on the proper time measurement, etc..

By introducing the tagging, the observed decay rates in the case that the final state f is a CP eigenstate take the form:

$$\Gamma_{B\to f}^{obs}(t) = (1 - \omega)\Gamma_{B\to f}(t) + \omega\Gamma_{\overline{B}\to f}(t) = \frac{|A_f|^2}{2}e^{-\Gamma t}\left[I_+(t) + (1 - 2\omega)I_-(t)\right]\tag{34}$$

and

$$\Gamma_{\overline{B}\to f}^{obs}(t) = \omega\Gamma_{B\to f}(t) + (1 - \omega)\Gamma_{\overline{B}\to f}(t) = \frac{|A_f|^2}{2}e^{-\Gamma t}\left[I_+(t) - (1 - 2\omega)I_-(t)\right],\tag{35}$$

where ω is the mistag probability.

In order to define a likelihood function it is very convenient to introduce a joint probability density function (p.d.f.) of the continuous variable t and the discrete variable q:

$$P(t,\, q) = \frac{e^{-\Gamma t}\left[I_+(t) + q(1 - 2\omega)I_-(t)\right]}{2\int e^{-\Gamma t'}I_+(t')dt'},\tag{36}$$

where q can take the discrete values 1 for events tagged as B, and -1 for events tagged as $\overline{B}$. It is trivial to check that this p.d.f. is correctly normalized to 1 by integrating on t and summing over the two discrete values of q. This joint p.d.f. is able to describe the whole sample of events tagged as B and $\overline{B}$ at the same time.

The generalization of the p.d.f. to the case where also the proper time resolution, the proper time acceptance, and the measured invariant mass are considered, is straightforward:

$$P(t,\, m,\, q) = \frac{\left\{e^{-\Gamma t'}\left[I_+(t') + q(1 - 2\omega)I_-(t')\right]\right\} \otimes R(t - t')\epsilon(t)G_S(m)}{2\int e^{-\Gamma t''}I_+(t'') \otimes R(\tau - t'')\epsilon(\tau)d\tau},\tag{37}$$

where the symbol $\otimes$ stands for convolution product, $R(t - t')$ is the proper time resolution function, $\epsilon(t)$ is the acceptance versus proper time and $G_S(m)$ is the p.d.f. of the invariant mass.

The inclusion of a component describing the combinatorial background further modifies the global p.d.f., which will assume the form:

Charmless charged two-body B decays at LHCb
Public Note
3 CP violation studies

Ref: *CERN-LHCb-2007-059*
Issue: *1*
Date: *September 8, 2007*

$$P(t,\, m,\, q) = f_S \frac{\left\{ e^{-\Gamma t'} \left[I_+(t') + q(1 - 2\omega)I_-(t') \right] \right\} \otimes R(t - t')\epsilon(t)G_S(m)}{2 \int e^{-\Gamma t''} I_+(t'') \otimes R(\tau - t'')\epsilon(\tau)d\tau} + \frac{1 - f_S}{2} B(t)G_B(m), \quad (38)$$

being f_S the fraction of signal events, $B(t)$ and $G_B(m)$ effective p.d.f.s describing the shape of proper time and mass distributions of combinatorial background events. In this expression it has been assumed that the background is flavour tagging blind.

The case in which f is a flavour-specific final state is slightly more complicated by the fact that there are four observed decay rates, corresponding to the two flavour tagging categories times the two different final states. However, the expression of the p.d.f. can be kept in a compact form by introducing a further discrete variable r, which can assume the value 1 for the final state f, and -1 for the final state $\bar{f}$:

$$P(t,\, m,\, q,\, r) = f_S \frac{1 - r\mathcal{A}_{f,\bar{f}}}{2} \frac{\left\{ e^{-\Gamma t'} \left[I_+(t') + rq(1 - 2\omega)I_-(t') \right] \right\} \otimes R(t - t')\epsilon(t)G_S(m)}{2 \int e^{-\Gamma t''} I_+(t'') \otimes R(\tau - t'')\epsilon(\tau)d\tau} + \frac{1 - f_S}{4} B(t)G_B(m),$$
$$(39)$$

where $\mathcal{A}_{f,\bar{f}}$ is the charge asymmetry between the two final states, and we have assumed that the background is blind with respect to flavour tagging and final state.

It is worth mentioning that the above p.d.f.s can be easily used to describe also the untagged samples, simply by putting $\omega = 0.5$.

3.3 Likelihood functions

Having introduced the expressions of the p.d.f.s for the two cases of our interest, f CP eigenstate or flavour-specific state, the definition of the likelihood function is straightforward:

$$\mathcal{L}_{CP} = \prod_{i=1}^{N_{CP}} P(t_i,\, m_i,\, q_i), \tag{40}$$

$$\mathcal{L}_{non-CP} = \prod_{i=1}^{N_{non-CP}} P(t_i,\, m_i,\, q_i,\, r_i), \tag{41}$$

respectively for the two cases, where N_{CP} and N_{non-CP} are the total number of events in the samples (including background).

It is worth mentioning that, with the definition of the p.d.f.s given in the previous section, these likelihoods include both the information on the shape of the decay rates and the information of the integrals of the decay rates.

3.4 Relevant distributions to CP studies

We introduce now the quantitative details of the distributions which have still been left undefined, such as the proper time resolution, the proper time acceptance, the mistag probability, the shape of the invariant mass distribution of signal and background events, the shape of the time distribution for the background, etc..

Charmless charged two-body B decays at LHCb
Public Note
3   CP violation studies

Ref: *CERN-LHCb-2007-059*
Issue: *1*
Date: *September 8, 2007*
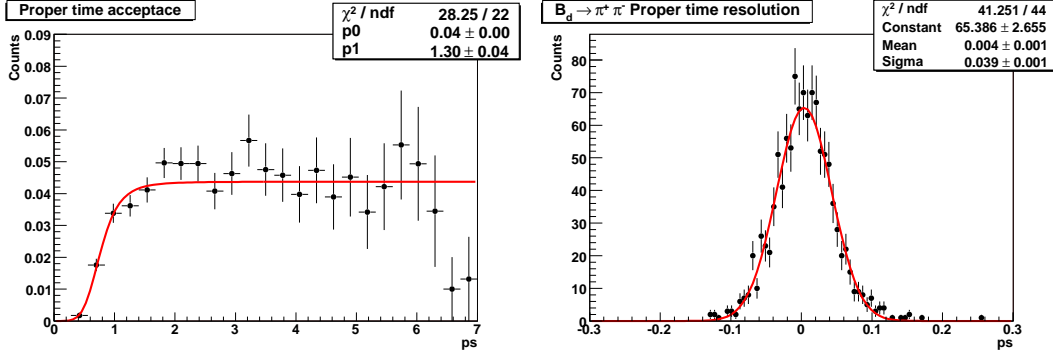
Figure 12 (a) Left: Proper time acceptance after trigger and offline selection for the $B_d \rightarrow \pi^+\pi^-$ decay. (b) Right: Proper time resolution for the $B_d \rightarrow \pi^+\pi^-$ decay.

Decay mode	α-fit (ps^{-1})
$B_d \rightarrow \pi^+\pi^-$	1.30 ±0.04
$B_d \rightarrow K^+\pi^-$	1.30±0.02
$B_s \rightarrow \pi^+K^-$	1.47±0.09
$B_s \rightarrow K^+K^-$	1.25±0.04
Mean	1.30±0.02

Table 11 Fit results for the α parameter of Eq. 42.

3.4.1   Proper time functions

The signal efficiency $\epsilon(t)$ as function of the proper time has been studied for each $B \rightarrow h^+h^-$ channel. As an example, the one corresponding to $B_d \rightarrow \pi^+\pi^-$ is shown in Fig. 12(a). It is well described by the following parameterization:

$$\epsilon(t) \propto \frac{(t\alpha)^5}{1 + (t\alpha)^5}. \tag{42}$$

Fit results for α are summarized in Tab. 11. The values for the different channels are consistent within the statistical errors, as expected.

As far as the proper time resolution function $R(t - t')$ is concerned, it turns out to be well described by a single Gaussian:

$$R(t - t') = \frac{1}{\sqrt{2\pi}\sigma} \exp\left(-\frac{(t - t')^2}{2\sigma^2}\right). \tag{43}$$

Fig. 12(b) shows the proper time distribution for the $B_d \rightarrow \pi^+\pi^-$ decay. A resolution of about 40 fs is obtained. The parameters σ obtained by fitting each decay mode are reported in Tab. 12. With more statistics and in a more realistic scenario, the proper time resolution can show other components than a simple Gaussian. A more refined work on the parameterization of the proper time distribution is under way (21).

The propertime resolution will be calibrated on data by using large samples of $J/\psi \rightarrow \mu^+\mu^-$ decays, collected through a dedicated di-muon trigger line thought not to introduce biases in the J/ψ proper time (22). Instead of using an average proper time resolution, one can make use use of the measurement of the proper time error on a per-event basis. As an example, Fig. 13 shows the distribution of the proper time error. This is a further improvement to the likelihood fit presented in this note, and is under study at the moment.

Charmless charged two-body B decays at LHCb
Public Note
3   CP violation studies

Ref: *CERN-LHCb-2007-059*
Issue: *1*
Date: *September 8, 2007*

Channel	σ-fit (ps)
$B_d \rightarrow \pi^+\pi^-$	0.039 $\pm$0.001
$B_d \rightarrow K^+\pi^-$	0.040$\pm$0.001
$B_s \rightarrow \pi^+K^-$	0.036$\pm$0.002
$B_s \rightarrow K^+K^-$	0.039$\pm$0.001

Table 12 Proper time resolution (width of single Gaussian).
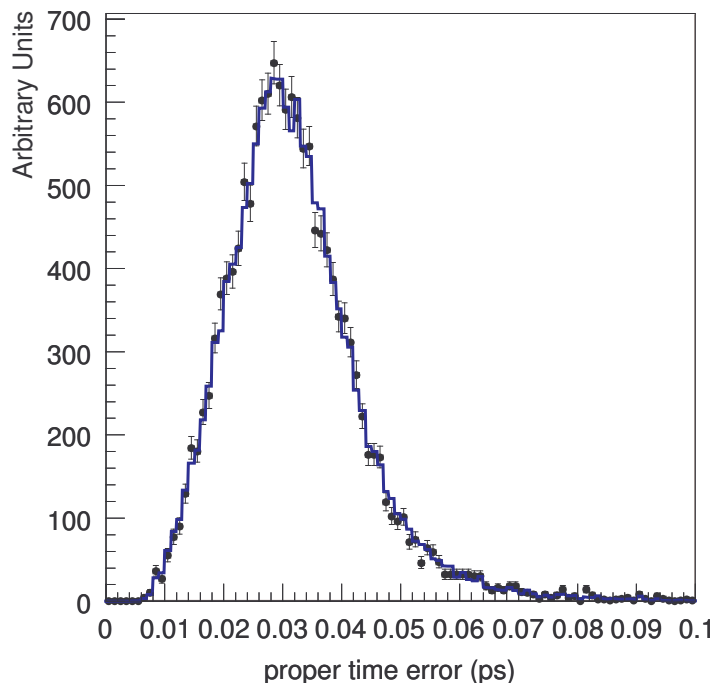
Figure 13 Distribution of proper time error for $B_d \rightarrow \pi^+\pi^-$ events.

The proper time distribution from selected $b\bar{b}$-inclusive events (excluding signal events present in the sample), for the $\pi^+\pi^-$ mass hypothesis, obtained after the offline selection in the mass window ± 600 around the nominal mass of the B-mesons, is shown in Fig. 14. In order to have a significant number of events we have not applied the trigger selection, but we can reasonably assume that the trigger does not change significantly the shape of the proper time distribution from $b\bar{b}$-inclusive events once the offline selection has been applied. When real data will be available, using the signal sidebands, the background proper time distribution will be very well determined.

The normalized rate $B(t)$ for $b\bar{b}$-inclusive events that fits to the data can be described by the function:

$$B\left(t\right) \propto e^{-\eta t} \cdot \frac{\left(\delta \cdot t\right)^5}{1 + \left(\delta \cdot t\right)^5}. \tag{44}$$

Tab. 13 shows the results of the fit for the $\pi^+\pi^-$ and $K^{\pm}\pi^{\mp}$ mass hypotheses. These were the only cases where a sufficient number of events survived the selection to allow a fit to the data to be performed. The values for the two mass hypotheses show an excellent agreement within the statistical errors.

Charmless charged two-body B decays at LHCb
Public Note
3 CP violation studies

Ref: *CERN-LHCb-2007-059*
Issue: *1*
Date: *September 8, 2007*
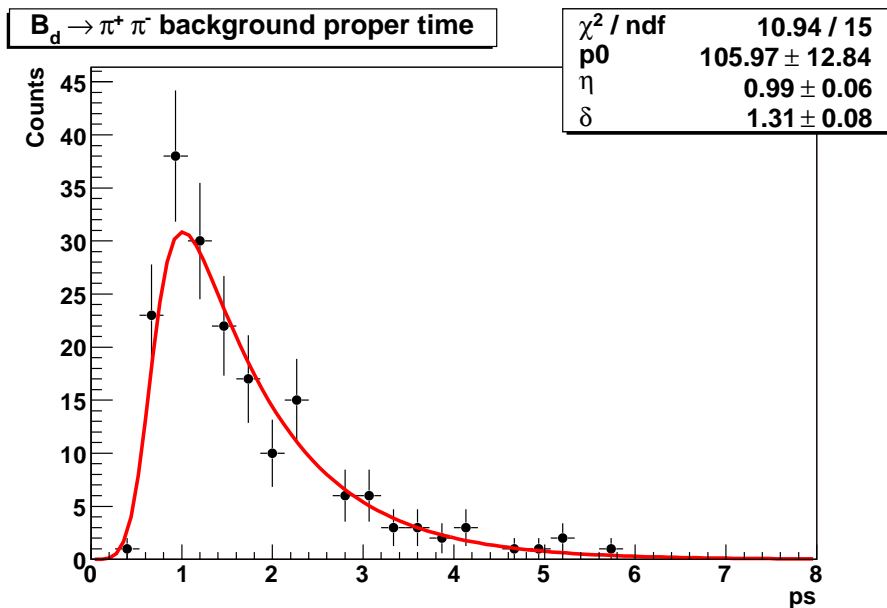
Figure 14 Proper time distribution from $b\bar{b}$-inclusive events for the $\pi^+\pi^-$ mass hypothesis, obtained by applying the selection within the mass window ± 600 MeV/c^2.

Mass hypothesis	η-fit (ps^{-1})	δ-fit (ps^{-1})
$\pi^+\pi^-$	0.99 $\pm$0.09	1.31 $\pm$0.08
$K^\pm\pi^\mp$	0.99 $\pm$0.14	1.31 $\pm$0.15
mean	0.99$\pm$0.08	1.31$\pm$0.07

Table 13 Results of the fit for the parameters entering the proper time distribution of $b\bar{b}$-inclusive events surviving the offline selection, for the mass hypotheses $\pi^+\pi^-$ and $K^\pm\pi^\mp$.

Charmless charged two-body B decays at LHCb
Public Note
3 CP violation studies

Ref: CERN-LHCb-2007-059
Issue: 1
Date: September 8, 2007
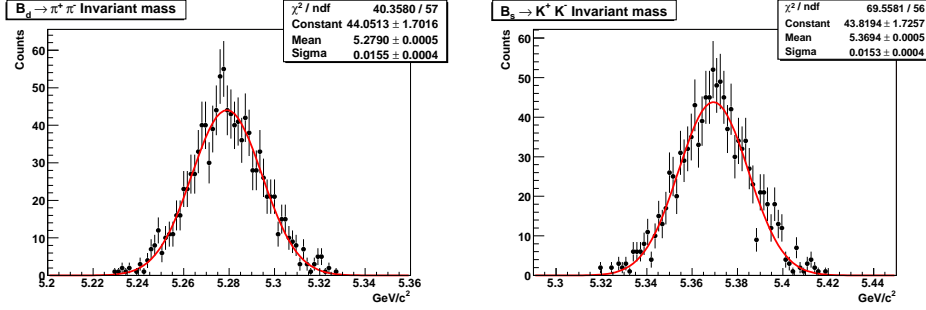
Figure 15 Invariant mass distributions of signal events surviving the offline selection and the trigger filter.

Channel	σ-fit (GeV/c^2)
$B_d \rightarrow \pi^+\pi^-$	0.0155 ±0.0004
$B_d \rightarrow K^+\pi^-$	0.0164 ±0.0002
$B_s \rightarrow \pi^+K^-$	0.016 ±0.001
$B_s \rightarrow K^+K^-$	0.0153 ±0.0004

Table 14 Summary of the invariant mass fit results.

3.4.2 Invariant mass distributions

The signal mass distribution for events surviving the trigger and the offline selection has been found to be consistent with a single Gaussian:

$$G_S(m) = \frac{1}{\sqrt{2\pi}\sigma_m} \exp\left(-\frac{(m - \overline{m})^2}{2\sigma_m^2}\right). \tag{45}$$

As an example, the distributions for the $B_d \rightarrow \pi^+\pi^-$ and $B_s \rightarrow K^+K^-$ are shown in Fig. 15. By fitting the distributions with a single Gaussian we obtain the results summarized in Tab. 14.

The combinatorial background mass distribution has been guessed to have an exponential shape:

$$g_B(m) \propto \exp(-\mu m), \tag{46}$$

with $m_{min} = 4.9\,GeV/c^2$ and $m_{max} = 5.7\,GeV/c^2$ the minimum and maximum mass values accepted by the trigger. This mass range is assumed to be available for the $B \rightarrow h^+h^-$ offline analyses. The value of μ, consistently amongst the various channels, has been determined from the full GEANT simulation to be $1.34 \pm 0.22\,c^2/GeV$.

3.4.3 Tagging efficiencies

A detailed description of the tagging algorithm can be found elsewhere (23). The statistical uncertainty on measured CP asymmetries is related to the effective tagging power ϵ_{eff} which is defined as:

$$\epsilon_{\text{eff}} = \epsilon_{tag}(1 - 2\omega)^2,$$

where ϵ_{tag} is the probability that the tagging algorithm gives an answer (tagging efficiency) and ω is the probability that the answer is wrong (wrong tagging fraction).

From the full GEANT simulation, we estimate for the $B_d \rightarrow \pi^+\pi^-$ and $B_d \rightarrow K^+\pi^-$ decays a tagging efficiency $\epsilon_{tag} \simeq 64\%$ and a mistag fraction $\omega \simeq 35\%$, leading to an effective tagging power of about 6%. For the $B_s \rightarrow K^+K^-$ and $B_s \rightarrow \pi^+K^-$ decays the values are $\epsilon_{tag} \simeq 60\%$ and $\omega \simeq 29\%$, resulting in an affective tagging power of about 10%. The larger effective tagging power in the B_s case is mainly

Charmless charged two-body B decays at LHCb
Public Note
3 CP violation studies

Ref: *CERN-LHCb-2007-059*
Issue: *1*
Date: *September 8, 2007*

due to the strength of the *same side kaon tagging*, which gives a relevant contribution only for the B_s channels.

As will be discussed in the next section, the calibration of the tagging power for $B \to h^+ h^{'-}$ modes will be performed on real data by using the flavour specific modes $B_d \to K^+\pi^-$ and $B_s \to \pi^+K^-$. Given the small branching ratio of the latter channel, in order to achieve a good statistical precision, other calibration channels might be employed as well.

A further improvement in the likelihood fit, not treated in this note but under study, might be given by the employment of a mistag fraction returned by means of a Neural Network approach on a per-event basis. In this case, a weight to each event is built according to its event-by-event mistag fraction. The p.d.f. for ω is built from the flavour-specific control samples. In order to employ the event-by-event mistag, Eq. 38 should be modified as:

$$P(t,\, m,\, q,\, \omega) = f_S \frac{\left\{ e^{-\Gamma t'}\left[I_+(t') + q(1 - 2\omega)I_-(t') \right] \right\} \otimes R(t - t')\epsilon(t)G_S(m)}{2\int e^{-\Gamma t''}I_+(t'') \otimes R(\tau - t'')\epsilon(\tau)d\tau} H(\omega) + \frac{1 - f_S}{2}B(t)G_B(m),$$

(47)

i.e. ω actually becomes an observable and $H(\omega)$ is the p.d.f. for ω, still assuming that the background is flavour tagging blind. One possible example of mistag distribution $H(\omega)$, obtained without including the vertex charge in the combination, is shown in Fig. 16.
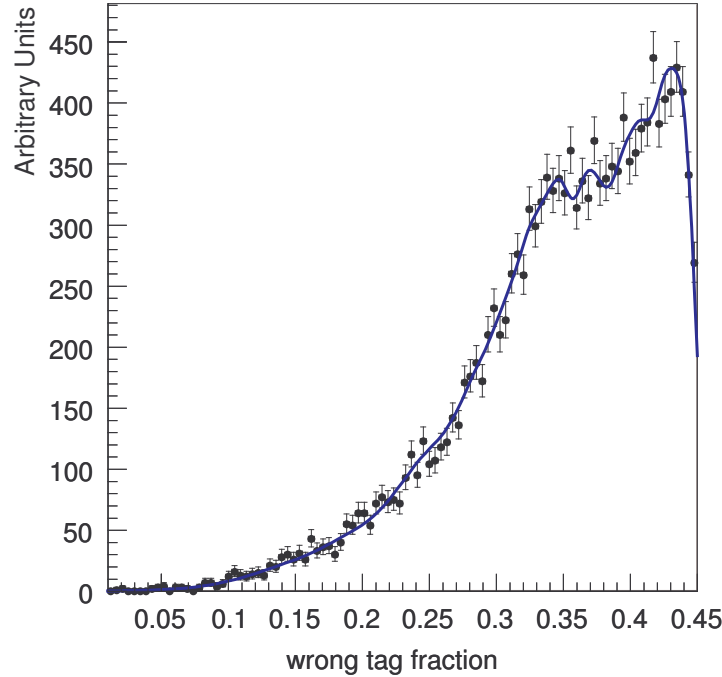

Figure 16 One possible example of the mistag distribution, obtained without including the vertex charge in the combination.

An alternative standard procedure we are implementing consists in separating the likelihood fit in different tagging categories, each one characterized by different (but fixed) values of the mistag probability.

Charmless charged two-body B decays at LHCb
Public Note
3   CP violation studies

Ref: *CERN-LHCb-2007-059*
Issue: *1*
Date: *September 8, 2007*

	$B_d \to \pi^+\pi^-$	$B_d \to K^+\pi^-$	$B_s \to \pi^+K^-$	$B_s \to K^+K^-$
Annual Event Yield	35700	137600	9800	35900
$\left(\frac{B}{S}\right)^{b\bar{b}}$	0.46	0.14	1.92	0.06
ϵ_{tag} [%]	64		60	
w [%]	35		29	
β	1.30			
$\sigma_{\Delta t}$ [fs]	39.1			
δ	1.31			
η [ps^{-1}]	0.99			
$\bar{m}$ [GeV/c^2]	5.279		5.369	
σ_m [GeV/c^2]	0.016			
μ [(GeV/c^2)$^{-1}$]	1.34			
τ [ps]	1.54		1.46	
$\Delta\Gamma$ [ps^{-1}]	0		0.0685	
Δm [ps^{-1}]	0.507		17.77	

Table 15 Values of the parameters used as inputs to the fast toy Monte Carlo simulation. For the meaning of the various terms see the text.

3.5   Sensitivity on CP observables

Having introduced in the previous sections the formalism needed to describe the time evolution of the decay rates, and consequently defined the relevant likelihood functions, we can now discuss the sensitivity achievable on the CP parameters of interest. This study includes the generation of fast Monte Carlo samples, parameterized and tuned according to the results obtained from the full GEANT simulation, and the subsequent unbinned maximum likelihood fits.

3.5.1   Fast Monte Carlo simulation

The data samples required to study the sensitivity on CP-violating observables for the $B \to h^+h^-$ decay channels have been generated by means of a fast toy Monte Carlo simulation based on the RooFit software framework (24). The program generates event-by-event proper time and mass values for triggered and offline-selected signal and combinatorial background events.

In the signal event generation, the effect of CP violation is obviously included, while no CP violation is assumed for the combinatorial background. The program also simulates the effect of the trigger and offline-selection acceptance as function of the proper time, the effect of the proper time resolution and the tagging.

All the input parameters used in the toy Monte Carlo generation, individually described in the previous sections, are summarized in Tab. 15. In the toy Monte Carlo study, the mass is generated from a value $m_{min} = 4.9\,GeV/c^2$ up to a value $m_{max} = 5.7\,GeV/c^2$, in order to include the mass sideband spectrum and simulate the extraction of the combinatorial background properties from data during the likelihood fit.

For the tagging of combinatorial background events, the same tagging efficiency of the signal is conservatively assumed, while the mistag probability is assumed to be 50% - i.e., one combinatorial background event can be randomly tagged as B or $\overline{B}$ with same probability.

As far as the central values of the CP-violating parameters used in the toy simulation are concerned, they are obtained from the current experimental measurements performed by BaBar (25), Belle (26) and more recently by CDF (1). In particular BaBar and Belle have measured the direct and mixing-induced CP parameters for the $B_d \to \pi^+\pi^-$ decay, and in addition the direct CP asymmetry of the $B_d \to K^+\pi^-$ decay. CDF has obtained the measurement of the direct CP asymmetry of the $B_d \to$

Charmless charged two-body B decays at LHCb   **Ref:** *CERN-LHCb-2007-059*
Public Note   **Issue:** *1*
3   CP violation studies   **Date:** *September 8, 2007*

	BaBar	Belle	CDF	Average
$\mathcal{A}_{\pi\pi}^{dir}$	$0.16 \pm 0.11 \pm 0.03$	$0.55 \pm 0.08 \pm 0.05$	-	0.39 ± 0.07
$\mathcal{A}_{\pi\pi}^{mix}$	$-0.53 \pm 0.14 \pm 0.02$	$-0.61 \pm 0.10 \pm 0.04$	-	-0.59 ± 0.09
$\mathcal{A}_{K\pi}$	$-0.108 \pm 0.025 \pm 0.008$	$-0.093 \pm 0.018 \pm 0.008$	$-0.058 \pm 0.039 \pm 0.007$	-0.093 ± 0.015

Table 16 Experimental knowledge of direct and mixing-induced CP parameters for $B_d \rightarrow \pi^-\pi^-$ and $B_d \rightarrow K^+\pi^-$ decays, as after Summer 2006 conferences (11). The sign convention of the various quantities is different from the one used by HFAG (see the text for the actual definition).

$\mathcal{A}_{KK}^{dir}$	-0.08 ± 0.03
$\mathcal{A}_{KK}^{mix}$	0.17 ± 0.04
$\mathcal{A}_{\pi K}$	0.39 ± 0.07

Table 17 Estimated values, according to U-spin symmetry, of the direct and mixing-induced CP parameters for $B_s \rightarrow K^-K^-$ and $B_s \rightarrow \pi^+K^-$ decays. The estimation is based on currently available experimental results. See Sec. 4 for details.

$K^+\pi^-$ decay, and very recently, for the first time, they are starting to reveal the direct CP asymmetry of the $B_s \rightarrow K^-\pi^+$ decay. Furthermore, CDF has collected significant samples of $B_d \rightarrow \pi^+\pi^-$ and $B_s \rightarrow K^+K^-$ decays, hence they will have soon first measurements of direct and mixing-induced CP parameters for these decays as well.

The experimental knowledge and the averages by HFAG (11), as after summer 2006 conferences, is reported in Tab. 16.

It is worth noting that the agreement between the measurements of the direct CP term of the $B_d \rightarrow \pi^+\pi^-$ decay between BaBar and Belle is not very satisfactory at present. In order to draw definitive conclusions in the interpretation of the data it is still very important to solve the tension between the two values.

In order to complete the picture, we need to fix also the values of the CP observables for the still un-measured B_s sector. To this aim we assume the validity of the U-spin symmetry, as described in ref. (27). Before proceeding with estimating the numerical values, we need however to introduce additional formalism and techniques, and this will be done in Sec. 4. For convenience we report here in advance the estimated values, see Tab. 17.

3.5.2   Likelihood fits and results

Once the fast Monte Carlo samples have been generated, unbinned maximum likelihood fits are performed to determine best values and errors of all the input parameters of the toy Monte Carlo generation, in particular of the CP-violating ones. The fits are performed on both tagged and untagged samples. Due to the statistical fluctuations in the samples, the sequence generation-fit is performed several times with different random seeds. This allows the determination of the average errors, as well as to verify by studying the pull distributions the correctness of the fitting procedure.

The unbinned maximum likelihood fits are performed by using the RooFit package. We have also checked that the RooFit results are exactly reproduced by a home-made fitting FORTRAN code, described in ref. (28). RooFit provides an advanced C++ interface to define the relevant likelihood functions and compose them by means of a sophisticated and complete abstraction language. As the underlying fitting algorithm, it then employs the MINUIT package (29).

By looking at the experimental CP asymmetry for the $B_d \rightarrow \pi^+\pi^-$ decay that, in the case of no background and perfect proper time resolution for simplicity, can be written as:

$$\mathcal{A}_{\pi\pi}^{CP}(t) = (1 - 2\omega)\left(\mathcal{A}_{\pi\pi}^{dir}\cos\Delta m_d\, t + \mathcal{A}_{\pi\pi}^{mix}\sin\Delta m_d\, t\right), \qquad (48)$$

Charmless charged two-body B decays at LHCb **Ref:** *CERN-LHCb-2007-059*
Public Note **Issue:** *1*
3 CP violation studies **Date:** *September 8, 2007*

one can easily understand that it is not possible to extract ω, $\mathcal{A}_{\pi\pi}^{dir}$ and $\mathcal{A}_{\pi\pi}^{mix}$ simultaneously from the $B_d \to \pi^+\pi^-$ data only: the problem is underconstrained.

However, considering that the $B_d \to K^+\pi^-$ decay is topologically identical to the $B_d \to \pi^+\pi^-$ decay - apart from small systematic effects that can be taken into account - one expects for the two channels to have the same mistag probability. For the $B_d \to K^+\pi^-$ decay, two experimental decay asymmetries can be written, given by:

$$\mathcal{A}_{K^+\pi^-}(t) = -(1 - 2\omega)\cos\Delta m_d\, t \tag{49}$$

and

$$\mathcal{A}_{K^-\pi^+}(t) = (1 - 2\omega)\cos\Delta m_d\, t. \tag{50}$$

It is clear that from the $B_d \to K^+\pi^-$ decay alone it is possible to extract the mistag probability ω from data. Thus one can determine the mistag probability from the $B_d \to K^+\pi^-$ sample, i.e. using it as a control channel, and reuse ω in the $B_d \to \pi^+\pi^-$ fit to unambigously extract the direct and mixing-induced CP terms.

Analogous consideration holds in the case of the $B_s \to K^+K^-$ and $B_s \to \pi^+K^-$ decays, with the only caveat that the statistics available in one year for the $B_s \to \pi^+K^-$ decay is much smaller with respect to the other decays. In this case, in order to determine ω with good precision, it could be necessary to use topologically different control channels, like $B_s \to D_s\pi$ or $B_s \to D_s\mu\nu$, but using particular experimental techniques allowing to minimize the differences introduced by the different trigger and the offline selection. For simplicity this case is not treated in this note.

Instead of performing separate fits, the first to determine ω and the second one to determine the CP asymmetry terms of the CP eigenstate, it is convenient to perform a combined likelihood fit of both the samples. This is also because some parameters, like the ones describing the mass distribution of the signal events, are the same in the two samples, and thus the statistical precision can be enhanced. The combined likelihood function is obtained simply by multiplying the two likelihoods each-other. The likelihood fits have been performed using both the tagged and untagged samples.

In order to obtain the best sensitivities on the CP-violating observables, it is still important to introduce a further ingredient. In the case of the $B_d \to \pi^+\pi^-$ and $B_d \to K^+\pi^-$ combined fit we can exploit existing prior information, such as the known resolution and values of Δm_d and Γ_d. These information can be naturally included in the fit by multiplying the likelihood by Gaussian functions, which play the role of "penalties" to the likelihood:

$$\log\mathcal{L}'_{\pi\pi,\,K\pi} = \log\mathcal{L}_{\pi\pi,\,K\pi} - \frac{(\Delta m_d - \overline{\Delta m_d})^2}{2\sigma_{\Delta m_d}^2} - \frac{(\Gamma_d - \overline{\Gamma}_d)^2}{2\sigma_{\Gamma_d}^2}. \tag{51}$$

For $\sigma_{\Delta m_d}$ and σ_{Γ_d}, their current knowledge has been used (30). No prior information on $\Delta\Gamma_d$ has been used.

For the $B_s \to K^+K^-$ and $B_s \to \pi^+K^-$ combined fit, prior information on $\Delta\Gamma_s$, Δm_s and Γ_s are included:

$$\log\mathcal{L}'_{KK,\,\pi K} = \log\mathcal{L}_{KK,\,\pi K} - \frac{(\Delta\Gamma_s - \overline{\Delta\Gamma}_s)^2}{2\sigma_{\Delta\Gamma_s}^2} - \frac{(\Delta m_s - \overline{\Delta m_s})^2}{2\sigma_{\Delta m_s}^2} - \frac{(\Gamma_s - \overline{\Gamma}_s)^2}{2\sigma_{\Gamma_s}^2}. \tag{52}$$

For $\sigma_{\Delta\Gamma_s}$ and σ_{Γ_s}, the expected sensitivities from the LHCb $B_s \to J/\psi\phi$ analysis have been used (31), while for $\sigma_{\Delta m_s}$ we employ the expectations of the LHCb $B_s \to D_s\pi$ analysis (32).

As an example, Fig. 17 shows the proper time distribution generated by one toy Monte Carlo run, corresponding to a sample of $B_s \to K^+K^-$ events tagged as B and an integrated luminosity of $2\,fb^{-1}$, with the result of the likelihood fit superimposed.

The average statistical sensitivities on $\mathcal{A}_{\pi\pi}^{dir}$, $\mathcal{A}_{\pi\pi}^{mix}$ and the charge asymmetry $\mathcal{A}_{K\pi}$ as well as the respective B_s ones, corresponding to an integrated luminosity of $2\,fb^{-1}$, are summarized in the Tab. 18.
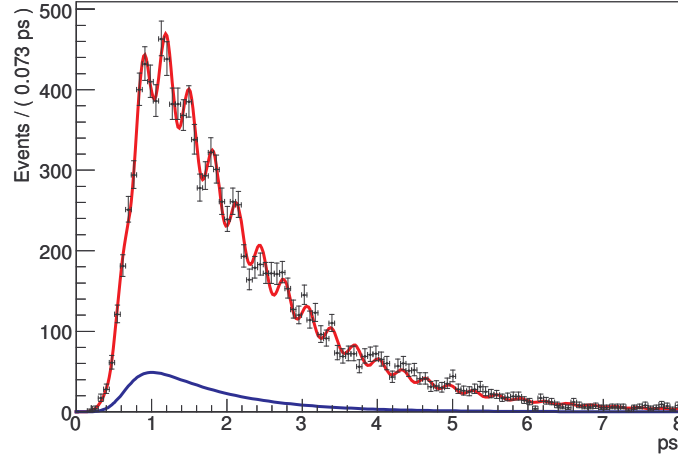
Charmless charged two-body B decays at LHCb
Public Note
4   U-spin symmetry studies and extraction of γ

Ref: *CERN-LHCb-2007-059*
Issue: *1*
Date: *September 8, 2007*

Figure 17 Proper time distribution generated by one toy Monte Carlo run, corresponding to a sample of $B_s \to K^+ K^-$ events tagged as B and an integrated luminosity of $2 fb^{-1}$. The curve superimposed to the data points represents the projection of the result of the likelihood fit. The lower curve is just the contribution of the background. In this example the value of Δm_s used in the generation was $20 \ ps^{-1}$, slightly larger than the one measured by CDF (33), which has been used as default input value to the toy Monte Carlo, as described in the text.

$\sigma(\mathcal{A}_{\pi\pi}^{dir})$	0.043	$\sigma(\mathcal{A}_{KK}^{dir})$	0.042
$\sigma(\mathcal{A}_{\pi\pi}^{mix})$	0.037	$\sigma(\mathcal{A}_{KK}^{mix})$	0.044
$\sigma(\mathcal{A}_{K\pi})$	0.003	$\sigma(\mathcal{A}_{\pi K})$	0.02

Table 18 Average statistical uncertainties on the relevant CP-violating observables of the $B \to h^+ h'^-$ decays, corresponding to one year of data ($2 fb^{-1}$ of integrated luminosity).

4   U-spin symmetry studies and extraction of γ

4.1   CP violation in $B \to h^+ h^-$ decays

The decay $B_d \to \pi^+ \pi^-$ is generated by the $\overline{b} \to \overline{u} + W^+$ tree diagram, as well as by $\overline{b} \to \overline{d} + g \left(\gamma, \ Z^0 \right)$ penguin diagrams. Analogously, the $B_s \to K^+ K^-$ is generated by the same diagrams, if all the $d \ (\overline{d})$ quarks are replaced by the $s \ (\overline{s})$ quarks (see Fig. 18). Concerning the $B_d \to K^+ \pi^-$ and $B_s \to \pi^+ K^-$ decays, it can be noted that they differ only in the spectator quarks from $B_s \to K^+ K^-$ and $B_d \to \pi^+ \pi^-$ respectively, as far as the tree and penguin diagrams are concerned. However, there are other decay topologies which are present in the case of $B_d \to \pi^+ \pi^-$ and $B_s \to K^+ K^-$, i.e. exchange and annihilation ones, but absent in the case of $B_d \to K^+ \pi^-$ and $B_s \to \pi^+ K^-$ (27). In addition to the U-spin symmetry, it is then needed to consider further dynamical assumptions (i.e. that exchange and annihilation diagrams give negligible contributions with respect to tree and penguin ones) in order to establish a direct link between them.

The direct and mixing-induced CP asymmetry terms for the $B_d \to \pi^+ \pi^-$ decay can be parametrized in the Standard Model as (27; 34):

$$\mathcal{A}_{\pi\pi}^{dir} = \mathcal{A}_{\pi\pi}^{dir}(d, \vartheta, \gamma) = \frac{2d \sin \vartheta \sin \gamma}{1 - 2d \cos \vartheta \cos \gamma + d^2} \tag{53}$$
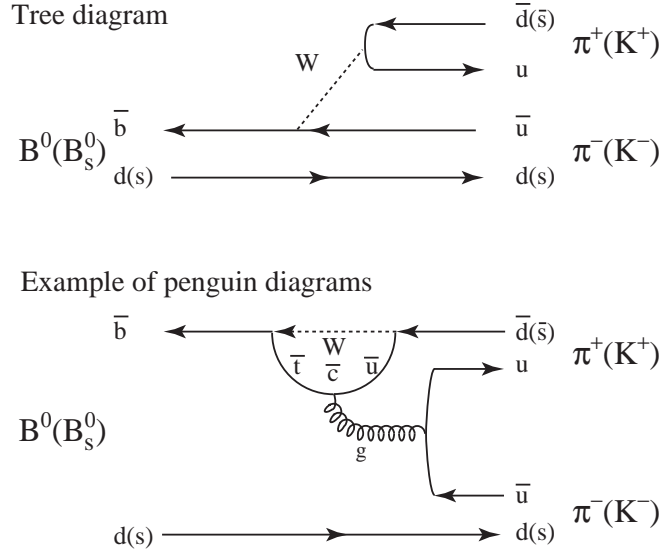
and

Charmless charged two-body B decays at LHCb
Public Note
4   U-spin symmetry studies and extraction of γ

Ref: *CERN-LHCb-2007-059*
Issue: *1*
Date: *September 8, 2007*

Tree diagram

Example of penguin diagrams

Figure 18 Tree and penguin diagrams generating $B_d \to \pi^+\pi^-$ ($B_s \to K^+K^-$) decays. By exchanging all the d ($\overline{d}$) quarks by the s ($\overline{s}$) quarks, the tree and penguin processes of the $B_d \to \pi^+\pi^-$ generate those of the $B_s \to K^+K^-$.

$$\mathcal{A}_{\pi\pi}^{mix} = \mathcal{A}_{\pi\pi}^{mix}(d,\,\vartheta,\,\gamma,\,\phi_d) = -\frac{\sin(\phi_d + 2\gamma) - 2d\cos\vartheta\sin(\phi_d + \gamma) + d^2\sin\phi_d}{1 - 2d\cos\vartheta\cos\gamma + d^2}, \tag{54}$$

where the dependence on the CKM angle γ is made explicit, and $\phi_d = 2\beta$ is the $B_d - \overline{B}_d$ mixing phase, experimentally well known nowadays from the BaBar and Belle measurements (35; 36). The parameters d and ϑ are real quantities defined by:

$$de^{i\vartheta} = \frac{1}{R_b}\frac{P^c - P^t}{T^u + P^u - P^t}, \tag{55}$$

where P^j ($j \in \{u,\,c,\,t\}$) describe penguin topologies with internal j quarks, and T^u describes current-current contributions. The factor R_b is one of the sides of the Unitarity Triangle, given by:

$$R_b = \frac{1}{\lambda}\left(1 - \frac{\lambda^2}{2}\right)\left|\frac{V_{ub}}{V_{cb}}\right|, \tag{56}$$

where λ is the sine of the Cabibbo angle.

For the $B_s \to K^+K^-$ channel, following similar lines, one can write:

$$\mathcal{A}_{KK}^{dir} = \mathcal{A}_{KK}^{dir}(d',\,\vartheta',\,\gamma) = -\frac{2\tilde{d}'\sin\vartheta'\sin\gamma}{1 + 2\tilde{d}'\cos\vartheta'\cos\gamma + \tilde{d}'^2}, \tag{57}$$

$$\mathcal{A}_{KK}^{mix} = \mathcal{A}_{KK}^{mix}(d',\,\vartheta',\,\gamma,\,\phi_s) = -\frac{\sin(\phi_s + 2\gamma) + 2\tilde{d}'\cos\vartheta'\sin(\phi_s + \gamma) + \tilde{d}'^2\sin\phi_s}{1 + 2\tilde{d}'\cos\vartheta'\cos\gamma + \tilde{d}'^2} \tag{58}$$

where $\phi_s = -2\beta_s$ is the $B_s - \overline{B}_s$ mixing phase and the parameter $\tilde{d}'$ is defined as:

$$\tilde{d}' = \frac{1 - \lambda^2}{\lambda^2}d'. \tag{59}$$

d' and ϑ' are the analogs of d and ϑ for the $B_s \to K^+K^-$ decay, similarly defined by:

Charmless charged two-body B decays at LHCb
Ref: CERN-LHCb-2007-059
Public Note
Issue: 1
4 U-spin symmetry studies and extraction of γ
Date: September 8, 2007

$$d' e^{i\vartheta'} = \frac{1}{R_b} \frac{P'^c - P'^t}{T'^u + P'^u - P'^t}. \tag{60}$$

By noting that the $B_d \to \pi^+\pi^-$ and $B_s \to K^+K^-$ decays are each other related by exchanging all the d $(\bar{d})$ and the s $(\bar{s})$ quarks, in the limit of validity of the U-spin symmetry of the strong interaction dynamics, one can write:

$$d = d' \tag{61}$$

and

$$\vartheta = \vartheta'. \tag{62}$$

Finally, since the tree and penguin diagrams of the $B_d \to K^+\pi^-$ and $B_s \to \pi^+K^-$ decays differ only in the spectator quarks from $B_s \to K^+K^-$ and $B_d \to \pi^+\pi^-$ decays, respectively, by relying on the U-spin flavor symmetry and on certain dynamical assumptions (27; 34), one can write the following relations:

$$\mathcal{A}_{KK}^{dir} \simeq \mathcal{A}_{K\pi} \tag{63}$$

and

$$\mathcal{A}_{\pi\pi}^{dir} \simeq \mathcal{A}_{\pi K}, \tag{64}$$

where $\mathcal{A}_{K\pi}$ is the charge asymmetry for the $B_d \to K^+\pi^-$ decay, and $\mathcal{A}_{\pi K}$ is the charge asymmetry for the $B_s \to \pi^+K^-$ decay.

4.2 Extraction of the γ angle

Assuming measurements have been made of $\mathcal{A}_{\pi\pi}^{dir}$, $\mathcal{A}_{\pi\pi}^{mix}$, $\mathcal{A}_{KK}^{dir}$ and $\mathcal{A}_{KK}^{mix}$, equations 53, 54, 57 and 58 constitute a system of 4 equations with 7 unknowns: d, ϑ, ϕ_d, γ, d', ϑ' and ϕ_s. However, ϕ_d is already well measured, and ϕ_s will be measured by LHCb with comparable precision to ϕ_d by means of the $B_s \to J/\psi\phi$ decay. By further employing the U-spin symmetry, i.e. the identities 61 and 62, one remains with just 3 unknowns, and the system is overconstrained and solvable. Hence it is possible to determine simultaneously d, ϑ and γ.

4.2.1 γ from present $B \to h^+h'^-$ measurements

At present, just $\mathcal{A}_{\pi\pi}^{dir}$, $\mathcal{A}_{\pi\pi}^{mix}$ and $\mathcal{A}_{K\pi}$ are experimentally known (see Tab. 16), thus it is not possible yet to employ the full method. However, a variant of the method consists in the employment of Eq. 63. In fact it allows to estimate - although with the additional requirement of certain dynamical assumptions, absent in the full method - the value of $\mathcal{A}_{KK}^{dir}$. In this case one can end up with 3 equations and 3 unknowns, but assuming for ϕ_s the Standard Model expectation, being ϕ_s still unmeasured with sufficient precision. It is then interesting to check what one would obtain by just using the currently available measurements, in particular whether the extracted value of γ agrees with the indirect prediction from Unitarity Triangle fits (37), $\gamma = (64.6 \pm 4.2)°$.

The problem to solve consists in inferring a joint p.d.f. for d, ϑ and γ from the p.d.f.s of $\mathcal{A}_{\pi\pi}^{dir}$, $\mathcal{A}_{\pi\pi}^{mix}$ and $\mathcal{A}_{K\pi}$ obtained from the experiments. Without going into technical details, that can be found in the literature (38), to this end we make use of a Bayesian approach implemented in the software packages developed by the UTfit Collaboration (37).
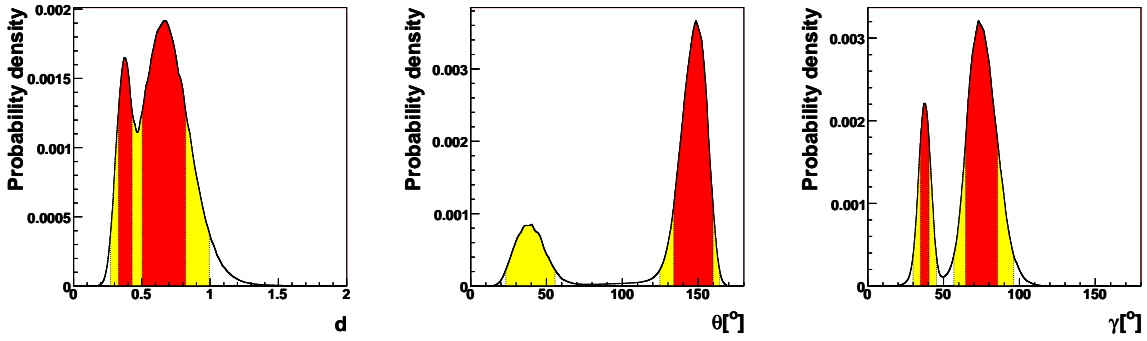
Charmless charged two-body B decays at LHCb **Ref:** *CERN-LHCb-2007-059*
Public Note **Issue:** *1*
4   U-spin symmetry studies and extraction of γ **Date:** *September 8, 2007*

Figure 19 From left to right: p.d.f.s for d, ϑ and γ obtained by using the current experimental measurements.
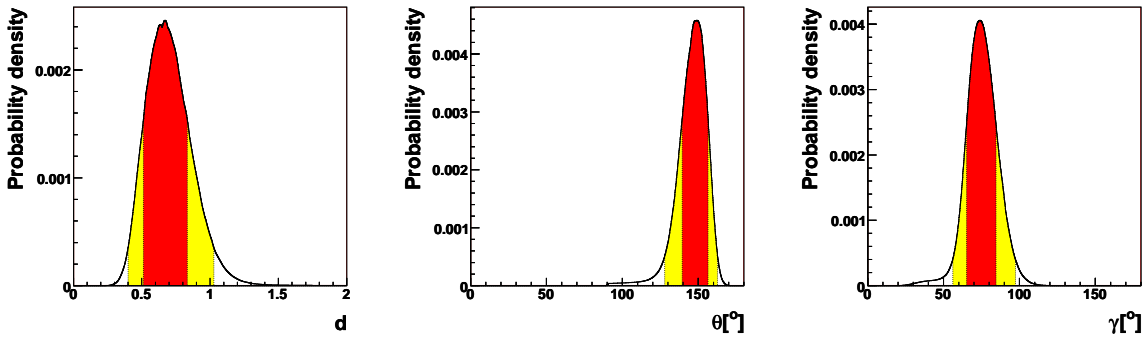

Figure 20 From left to right: p.d.f.s for d, ϑ and γ obtained by using the current experimental measurements, and imposing a *prior* $\vartheta > 90°$ in order to isolate the Standard Model solution.

In order not to fully rely on the validity of the U-spin symmetry, we allow in the Bayesian treatment for a breaking of the U-spin relations 61 and 62 of 20% and $\pm 20°$ respectively, i.e. ξ and $\Delta\vartheta$ are varied uniformly in the ranges[5]:

$$\xi = d'/d \in [0.8,\ 1.2], \tag{65}$$

and

$$\Delta\vartheta = \vartheta' - \vartheta \in [-20°,\ 20°]. \tag{66}$$

The individual p.d.f.s for d, ϑ and γ that we determine this way, obtained by integrating out from the joint p.d.f. the other two variables in turn, are shown in Fig. 19. Due to the non-linearity of the system of equations, it is evident from the plots that two solutions are present. The Standard Model solution can be easily isolated by putting a *prior* on the ϑ variable, e.g. imposing $\vartheta > 90°$, since the two solutions are very well separated in ϑ. By doing so, one obtains the p.d.f.s shown in Fig. 20. The corresponding central values and 68% probability intervals are reported in Tab. 19. The result shows an excellent agreement, within experimental errors, of the value of γ with the indirect determination from Unitarity Triangle fits. Furthermore it gives numerical estimates of the hadronic parameters

---

[5]When this note was almost completed, a paper on the same subject discussed in this section, written by the original author of the strategy we are employing, became available (39). In that paper, the author allows for a breaking of 15% and $\pm 20°$ on d and ϑ respectively.

Charmless charged two-body B decays at LHCb
Public Note
4 U-spin symmetry studies and extraction of γ

Ref: *CERN-LHCb-2007-059*
Issue: *1*
Date: *September 8, 2007*

d	ϑ	γ
0.67 ± 0.16	$(148 \pm 9)°$	$(75 \pm 10)°$

Table 19 Central values and 68% probability intervals for d, ϑ and γ, corresponding to the Standard Model solution (see text), obtained by using the current experimental measurements.

d and ϑ, that can be used to drive theory in correctly modelling the underlying hadron dynamics involved in the decays under study.

With the determined values of d, ϑ and γ we can predict the values of $\mathcal{A}_{KK}^{dir}$ and $\mathcal{A}_{KK}^{mix}$ by assuming the validity of the U-spin symmetry and using equations 57 and 58. Finally, for completing the picture, a prediction for $\mathcal{A}_{\pi K}$ can be easily obtained by means of Eq. 64. All the numerical values have already been reported for convenience previously in Tab. 17.

4.2.2 γ from $B \to h^+ h'^-$ decays at LHCb

Differently from the previous case, LHCb will measure all the 4 CP-violating observables $\mathcal{A}_{\pi\pi}^{dir}$, $\mathcal{A}_{\pi\pi}^{mix}$, $\mathcal{A}_{KK}^{dir}$ and $\mathcal{A}_{KK}^{mix}$, thus it will not need to rely on any dynamical assumption to perform the extraction of γ. Moreover, having one more constraint equation to employ, it is not strictly necessary to rely on the two U-spin symmetry equations 61 and 62, but is sufficient to use just one of the two, hence being less dependent on the U-spin assumption.

In our study we have used just Eq. 61, i.e. we have left ϑ and ϑ' free and independent. Moreover we have taken into account a 20% breaking effect on ξ. By fitting ϑ and ϑ' independently, we can also extract the value of their difference $\Delta\vartheta$, i.e. we can get a measurement of the U-spin breaking on the strong phase from data itself. The validity of the U-spin symmetry will be confirmed if and only if $\Delta\vartheta$ will be compatible with zero. We could also have chosen Eq. 62 as the U-spin relation to employ, and fitted independently d and d' instead. However in this note we just report for simplicity the results obtained in the former case.

Fig. 21 shows the p.d.f.s for d, ϑ, $\Delta\vartheta$ and γ, obtained by assuming the errors on the CP-violating observables reported in Tab. 18, i.e. corresponding to $2\,fb^{-1}$ of integrated LHCb luminosity. The respective sensitivities for the Standard Model solution are summarized in Tab. 20.

d	ϑ	$\Delta\vartheta$	γ
0.18	9°	17°	10°

Table 20 Sensitivities (calculated as halves of the 68% probability intervals) for d, ϑ, $\Delta\vartheta$ and γ, corresponding to $2\,fb^{-1}$ of LHCb integrated luminosity.

In order to show what we expect after an extended period of data taking, we also report in Fig. 22 and Tab. 21 the results for $10\,fb^{-1}$ of integrated luminosity.

d	ϑ	$\Delta\vartheta$	γ
0.09	5°	8°	5°

Table 21 Sensitivities (calculated as halves of the 68% probability intervals) for d, ϑ, $\Delta\vartheta$ and γ, corresponding to $10\,fb^{-1}$ of LHCb integrated luminosity.

Charmless charged two-body B decays at LHCb
Public Note
5 Conclusions

Ref: *CERN-LHCb-2007-059*
Issue: *1*
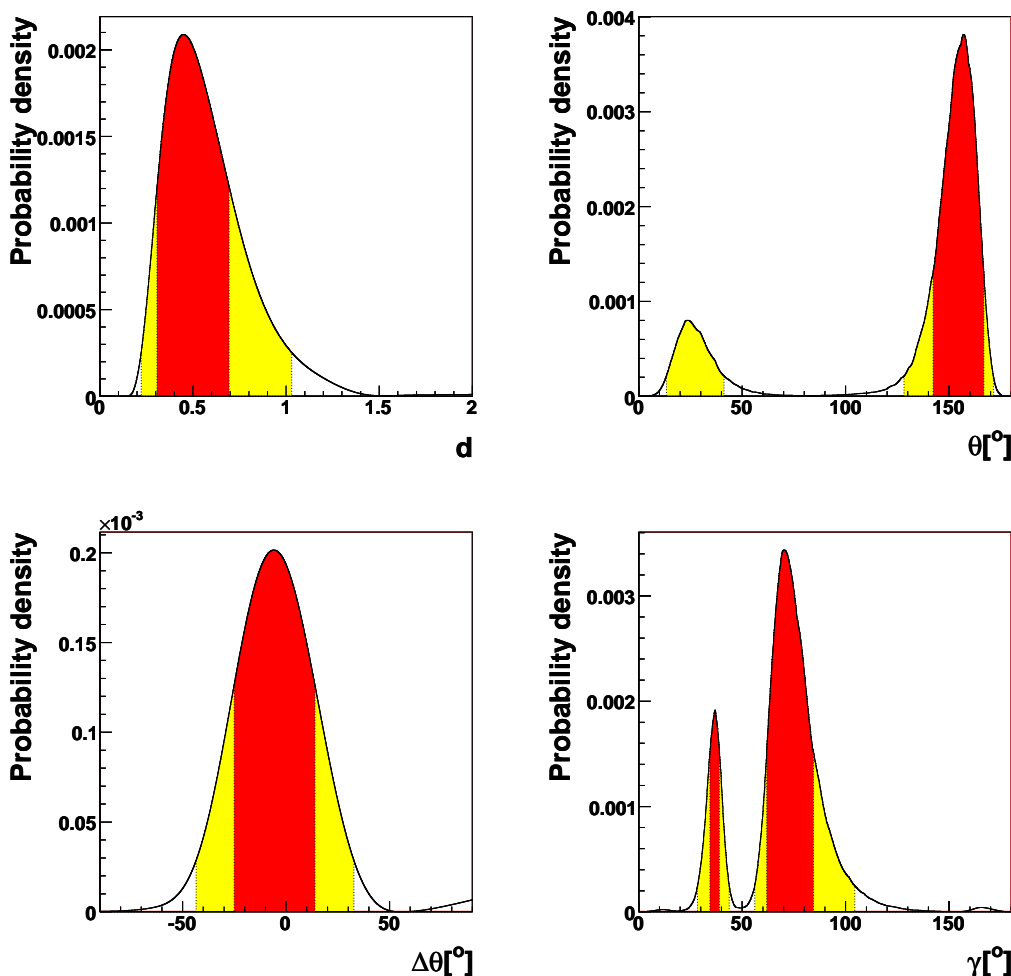Date: *September 8, 2007*

Figure 21 p.d.f.s for d (top left), ϑ (top right), $\Delta\vartheta$ (bottom left) and γ (bottom right) obtained by using LHCb measurements, corresponding to an integrated luminosity of $2\,fb^{-1}$.

5 Conclusions

We have presented the current status of the $B \to h^+h'^-$ analysis in LHCb, including the event selection and the extraction of the CP-violating observables from the selected data samples. Due to the large statistics collected per year of data taking, it has been found that LHCb can realize very precise measurements of CP-violation for these decays.

The combination of the $B_d \to \pi^+\pi^-$ and $B_s \to K^+K^-$ CP measurements can be used to extract the CKM phase γ (27), relying on the validity of the U-spin symmetry of the strong interaction dynamics. An implementation of this method, based on a Bayesian approach, has been realized, and the resulting sensitivity on γ has been estimated.

The relevance of this measurement can be made immediately visible considering that, since both $\overline{b} \to \overline{d} + g\left(\gamma, Z^0\right)$ and $\overline{b} \to \overline{s} + g\left(\gamma, Z^0\right)$ penguin processes are involved in the $B_d \to \pi^+\pi^-$ and $B_s \to K^+K^-$ decay amplitudes, the value of γ determined in this way can be affected by sizable contributions from New Physics. This would lead to discrepancies with the values of γ predicted by the Standard Model through indirect Unitarity Triangle fits (37), as well as with those determined by using other B decays, such as $B_s \to D_s^{\mp}K^{\pm}$ (40), which is generated by pure $\overline{b} \to \overline{u} + W^+$ and
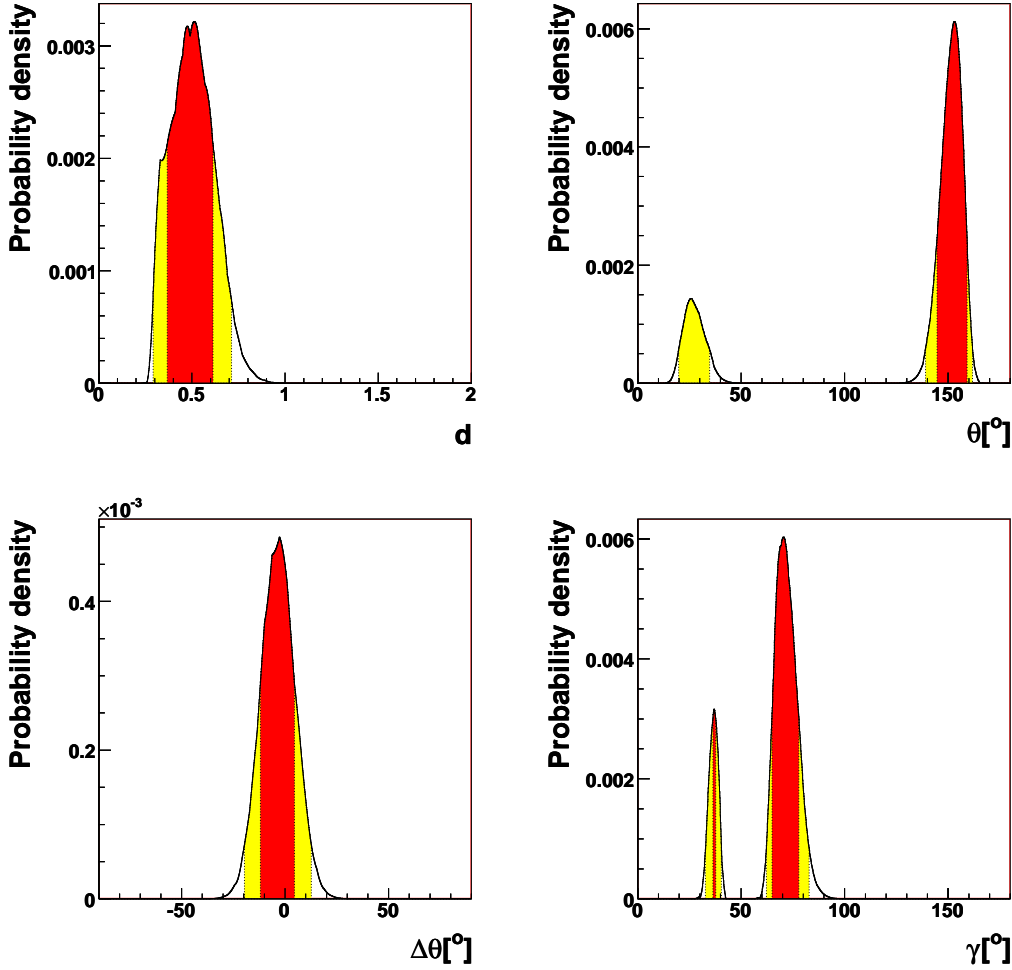
Charmless charged two-body B decays at LHCb
Public Note
5   Conclusions

Ref: *CERN-LHCb-2007-059*
Issue: *1*
Date: *September 8, 2007*

Figure 22 p.d.f.s for d (top left), ϑ (top right), $\Delta\vartheta$ (bottom left) and γ (bottom right) obtained by using LHCb measurements, corresponding to an integrated luminosity of $10\,fb^{-1}$.

$\bar{b} \to \bar{c} + W^+$ tree processes.

The work here presented is far from being complete. In particular we must still address the relevant systematic effects which affect the measurements, such as the presence of radiated photons in the final state, the charge asymmetries due to a different interaction of the final state particles with the detector, effects of incorrect proper time resolution, the limited knowledge of the proper time acceptance, systematics due to the tagging and production asymmetry, the effect of cross-feed backgrounds from the other $B \to h^+h'^-$ channels, the calibration of the particle identification, just to cite some of them.

Relevant improvements of the likelihood fits are under development, e.g. the combined fit of all the $B \to h^+h'^-$, in order to automatically take into account the already mentioned cross-feed backgrounds, the inclusion of particle identification variables in the likelihood fit, the employment of event-by-event proper time measurement and error and of event-by-event mistag fractions, the usage of event-by-event acceptance functions to be extracted from data itself, etc..

Furthermore, we still need to include in the analysis some important decay channels, like the very rare $B_d \to K^+K^-$ and $B_s \to \pi^+\pi^-$ ones, which proceed in the Standard Model through exchange and annihilation diagrams only, and are important ingredients for drawing the complete picture of $B \to h^+h'^-$ decays.

Charmless charged two-body B decays at LHCb
Public Note
5   Conclusions

Ref: *CERN-LHCb-2007-059*
Issue: *1*
Date: *September 8, 2007*

Acknowledgments

References

[1] A. Abulencia *et al.* [CDF Collaboration], Phys. Rev. Lett. **97** (2006) 211802 [arXiv:hep-ex/0607021].

[2] LHCb Collaboration, CERN-LHCC-2001-011.

[3] LHCb Collaboration, CERN-LHCC-2003-031.

[4] J. Closier *et al.*, Results of the LHCb experiment Data Challenge 2004, published in Proceedings of CHEP04 conference, Interlaken, Switzerland (2004).

[5] T. Sjostrand, S. Mrenna and P. Skands, JHEP **0605** (2006) 026 [arXiv:hep-ph/0603175].

[6] J. Allison *et al.*, IEEE Trans. Nucl. Sci. **53** (2006) 270.

[7] LHCb Gauss web page, http://cern.ch/LHCb-release-area/DOC/gauss.

[8] LHCb Boole web page, http://cern.ch/LHCb-release-area/DOC/boole.

[9] LHCb Brunel web page, http://cern.ch/LHCb-release-area/DOC/brunel.

[10] LHCb DaVinci web page, http://cern.ch/LHCb-release-area/DOC/davinci.

[11] E. Barberio *et al.* [Heavy Flavor Averaging Group],
http://www.slac.stanford.edu/xorg/hfag.

[12] LHCb RICH Group, CERN-LHCb-2004-121, CERN-LHCb-2002-009.

[13] LHCb Collaboration, CERN-LHCC-2000-037.

[14] LHCb Collaboration, CERN-LHCC-2000-036.

[15] LHCb Collaboration, CERN-LHCC-2001-029, CERN-LHCC-2003-002, CERN-LHCC-2005-012.

[16] LHCb Collaboration, CERN-LHCC-2003-030.

[17] J. Nardulli *et al.*, CERN-LHCb-2006-020.

[18] I. Mous, CERN-LHCb-2006-045.

[19] LHCb Collaboration, CERN-LHCC-2001-024.

[20] I. I. Bigi *et al.*, CP violation, ed. C. Jarlskog, Singapore World Scientific, 1989.

[21] P. Vankov, CERN-LHCb-2007-055.

[22] G. Balbi and S. Vecchi, CERN-LHCb-2007-056.

[23] M. Musy, M. Calvi and O. Leroy, CERN-LHCb-2007-058.

[24] W. Verkerke and D. Kirkby, *In the Proceedings of 2003 Conference for Computing in High-Energy and Nuclear Physics (CHEP 03), La Jolla, California, 24-28 Mar 2003, pp MOLT007* [arXiv:physics/0306116].

[25] B. Aubert *et al.* [BABAR Collaboration], arXiv:hep-ex/0607106.

[26] K. Abe [Belle Collaboration], arXiv:hep-ex/0608035.

[27] R. Fleischer, Phys. Lett. B **459** (1999) 306 [arXiv:hep-ph/9903456].

[28] V. Vagnoni *et al.*, CERN-LHCb-2003-124.

[29] F. James and M. Roos, Comput. Phys. Commun. **10** (1975) 343.

[30] W. M. Yao *et al.* [Particle Data Group], J. Phys. G **33** (2006) 1.

[31] L. Fernandez, CERN-LHCb-2006-047.

[32] J. Borel *et al.*, CERN-LHCb-2007-017.

[33] A. Abulencia *et al.* [CDF Collaboration], Phys. Rev. Lett. **97** (2006) 242003 [arXiv:hep-ex/0609040].

[34] R. Fleischer and J. Matias, Phys. Rev. D **66** (2002) 054009 [arXiv:hep-ph/0204101].

[35] B. Aubert *et al.* [BABAR Collaboration], arXiv:hep-ex/0703021.

[36] K. F. Chen *et al.* [Belle Collaboration], Phys. Rev. Lett. **98** (2007) 031802 [arXiv:hep-ex/0608039].

[37] M. Bona *et al.* [UTfit Collaboration], `http://www.utfit.org`.

[38] M. Ciuchini *et al.*, JHEP **0107** (2001) 013 [arXiv:hep-ph/0012308].

[39] R. Fleischer, arXiv:0705.1121 [hep-ph].

[40] S. Cohen, CERN-LHCb-2007-041.